This article is a *Plant Cell* Advance Online Publication. The date of its first appearance online is the official date of publication. The article has been edited and the authors have corrected proofs, but minor changes could be made before the final version is published. Posting this version online reduces the time to publication by several weeks.

LARGE-SCALE BIOLOGY ARTICLE

Arabidopsis Defense against *Botrytis cinerea*: Chronology and Regulation Deciphered by High-Resolution Temporal Transcriptomic Analysis[C][W]

Oliver Windram,[a,1,2] Priyadharshini Madhou,[a,1,3] Stuart McHattie,[b] Claire Hill,[a] Richard Hickman,[b,4] Emma Cooke,[c] Dafyd J. Jenkins,[b] Christopher A. Penfold,[b] Laura Baxter,[b] Emily Breeze,[a,b] Steven J. Kiddle,[b,5] Johanna Rhodes,[a] Susanna Atwell,[d] Daniel J. Kliebenstein,[d] Youn-sung Kim,[a,6] Oliver Stegle,[e] Karsten Borgwardt,[e,f] Cunjin Zhang,[a,7] Alex Tabrett,[a] Roxane Legaie,[b] Jonathan Moore,[b] Bärbel Finkenstadt,[g] David L. Wild,[b] Andrew Mead,[a] David Rand,[b] Jim Beynon,[a,b] Sascha Ott,[b] Vicky Buchanan-Wollaston,[a,b] and Katherine J. Denby[a,b,8]

[a] School of Life Sciences, University of Warwick, Coventry CV4 7AL, United Kingdom
[b] Warwick Systems Biology Centre, University of Warwick, Coventry CV4 7AL, United Kingdom
[c] Molecular Organization and Assembly of Cells Doctoral Training Centre, University of Warwick, Coventry CV4 7AL, United Kingdom
[d] Department of Plant Sciences, University of California, Davis, California 95616
[e] Max Planck Institute for Developmental Biology and Max Planck Institute for Intelligent Systems, 72076 Tuebingen, Germany
[f] Zentrum für Bioinformatik, Eberhard Karls Universität, 72076 Tuebingen, Germany
[g] Department of Statistics, University of Warwick, Coventry CV4 7AL, United Kingdom

Transcriptional reprogramming forms a major part of a plant's response to pathogen infection. Many individual components and pathways operating during plant defense have been identified, but our knowledge of how these different components interact is still rudimentary. We generated a high-resolution time series of gene expression profiles from a single *Arabidopsis thaliana* leaf during infection by the necrotrophic fungal pathogen *Botrytis cinerea*. Approximately one-third of the *Arabidopsis* genome is differentially expressed during the first 48 h after infection, with the majority of changes in gene expression occurring before significant lesion development. We used computational tools to obtain a detailed chronology of the defense response against *B. cinerea*, highlighting the times at which signaling and metabolic processes change, and identify transcription factor families operating at different times after infection. Motif enrichment and network inference predicted regulatory interactions, and testing of one such prediction identified a role for TGA3 in defense against necrotrophic pathogens. These data provide an unprecedented level of detail about transcriptional changes during a defense response and are suited to systems biology analyses to generate predictive models of the gene regulatory networks mediating the *Arabidopsis* response to *B. cinerea*.

[1] These authors contributed equally to this work.
[2] Current address: Centre for Synthetic Biology and Innovation, Division of Molecular Biosciences, Imperial College London, London SW7 2AZ, United Kingdom.
[3] Current address: Medical Research Council Centre for Developmental Neurobiology, King's College London, London SE1 1UL, United Kingdom.
[4] Current address: Department of Biology, Faculty of Science, Utrecht University, PO Box 800.56, 3508 TB Utrecht, The Netherlands.
[5] Current address: National Institute for Health Research Biomedical Research Centre for Mental Health, South London and Maudsley National Health Service Foundation Trust, London SE5 8AF, United Kingdom.
[6] Current address: Research Institute, GenDocs Inc. Yongsan-dong, Daejon 305-500, Republic of Korea.
[7] Current address: School of Biological and Biomedical Sciences, Durham University, Durham DH1 3LE, United Kingdom.
[8] Address correspondence to k.j.denby@warwick.ac.uk.
The author responsible for distribution of materials integral to the findings presented in this article in accordance with the policy described in the Instructions for Authors (www.plantcell.org) is: Katherine J. Denby (k.j.denby@warwick.ac.uk).
[C] Some figures in this article are displayed in color online but in black and white in the print edition.
[W] Online version contains Web-only data.
www.plantcell.org/cgi/doi/10.1105/tpc.112.102046

INTRODUCTION

Botrytis cinerea is considered the second most important fungal plant pathogen (Dean et al., 2012). Its broad host range and ability to cause disease both pre- and postharvest lead to large economic effects (both in terms of yield loss and cost of control). *B. cinerea* is a necrotrophic pathogen, meaning it kills plant tissue prior to feeding, and uses a range of toxic molecules (Williamson et al., 2007) as well as the plant's own defense mechanisms (Govrin et al., 2006) to destroy host cells.

Initial perception of plant pathogens is thought to occur by recognition of microbe-associated molecular patterns (MAMPs) and damage-associated molecular patterns (DAMPs) by host plant pattern recognition receptors (Boller and Felix, 2009). MAMPs (also known as pathogen-associated molecular patterns) are molecules or molecular tags that are essential for microbe viability and conserved between diverse genera; thus, they are unlikely to be lost through selection and are an efficient form of pathogen monitoring for the plant. DAMPs are signals generated by the plant in response to pathogen damage. MAMP

recognition by corresponding pattern recognition receptor triggers basal defense responses (known as pattern-triggered immunity), providing protection against nonhost pathogens and limiting disease caused by virulent pathogens (Jones and Dangl, 2006). Variation in multiple basal defense mechanisms is thought to underlie differences in host susceptibility to necrotrophic pathogens.

Multiple MAMPs are involved in the interaction between *B. cinerea* and *Arabidopsis thaliana*. The essential fungal cell wall component, chitin, and its constituent oligosaccharides are fungal MAMPs that activate numerous defense responses. Polygalacturonase (PG) is another component of *B. cinerea* that is essential for virulence and detected by the plant. PG is detected via at least two different mechanisms; one through its ability to function as a MAMP with the presence of the protein (independent of its enzymic activity) activating defense responses in the host (Poinssot et al., 2003). Additionally, PGs act on the host cell wall to degrade pectin, the primary carbon source for the pathogen, producing oligogalacturonides (OGs). OGs of a certain length (10 to 15 degrees of polymerization) are enriched by the action of plant PG-inhibiting proteins and function as DAMPs activating immunity against *B. cinerea* (Ferrari et al., 2007). A wall-associated kinase functions as a receptor for immunoactive OGs (Brutus et al., 2010), with intracellular mitogen-activated protein (MAP) kinase activity (MPK6) required for OG-induced resistance to *B. cinerea* (Galletti et al., 2011). A cytoplasmic receptor-like kinase, BIK1, is required for basal immunity against *B. cinerea* triggered by the bacterial MAMP flg22. BIK1 is part of the flg22 receptor complex and its action is dependent on ethylene (ET) signaling and histone monoubiquitination (Lu et al., 2010; Laluk et al., 2011). BIK1 also interacts with CERK1 (Zhang et al., 2010), suggesting it may play a similar role in pattern-triggered immunity triggered by chitin.

Signal transduction via plant hormones is another key component of basal immunity. Salicylic acid (SA) has been traditionally associated with defense against biotrophic pathogens (i.e., those that parasitize a living host), whereas jasmonic acid (JA) and ET signaling appear to be more important against necrotrophic pathogens (Thomma et al., 1998). This remains broadly true, although SA does appear to have a role in local immunity against *B. cinerea* (Ferrari et al., 2007). More crucially, we now know that there is extensive crosstalk between hormone pathways thought to enable the plant to fine-tune its defenses against specific pathogens (Verhage et al., 2010). Large-scale transcriptional reprogramming forms a major part of plant defense, and response to *B. cinerea* infection is no exception. Several studies have identified thousands of *Arabidopsis* transcripts that change in expression following *B. cinerea* infection (Ferrari et al., 2007; Rowe et al., 2010; Birkenbihl et al., 2012; Mulema and Denby, 2012), pointing to a major role for transcription factors (TFs) in coordinating these changes. Indeed, both forward and reverse genetic approaches have identified numerous TFs involved in defense against *B. cinerea*.

Two major groups of TFs with roles in defense against *B. cinerea* are the WRKY and ERF families. WRKYs are often associated with plant immunity and WRKY3, 4, 8, 18, 33, 40, 60, and 70 have all been shown to influence *B. cinerea* immunity (AbuQamar et al., 2006; Xu et al., 2006; Lai et al., 2008; Chen et al., 2010; Birkenbihl et al., 2012). *Arabidopsis* contains 122 ERFs, characterized by a single AP2/ERF DNA binding domain (Nakano et al., 2006). Expression of several of these, including ERF1, ERF5, ERF6, RAP2.2, and ORA59, influences host susceptibility to *B. cinerea*, with ERF5 a key component of chitin-mediated immunity (Berrocal-Lobo et al., 2002; Pré et al., 2008; Moffat et al., 2012; Son et al., 2012; Zhao et al., 2012). Members of the MYB and NAC families (Wang et al., 2009; Ramírez et al., 2011a) have also been shown to influence plant susceptibility to *B. cinerea*.

Despite this multitude of TFs affecting susceptibility to *B. cinerea*, very little is known about the regulatory network surrounding individual TFs with very few direct target genes or upstream regulators identified. An exception is WRKY33. Qiu et al. (2008) demonstrated that in uninfected leaves, WRKY33 is bound in a complex with MAP kinase 4 (MPK4) and MKS1. Infection with *Pseudomonas syringae* or treatment with flg22 activates MPK4, causing the release of WRKY33, which then enters the nucleus. Chromatin immunoprecipitation (ChIP)-PCR experiments have shown direct binding of WRKY33 to sequences upstream of genes involved in JA signaling (*jasmonate ZIM-domain1* [*JAZ1*] and *JAZ5*), ET-JA crosstalk (*ORA59*), and camalexin biosynthesis (*PAD3* and *CYP71A13*) following *B. cinerea* infection (Birkenbihl et al., 2012). WRKY33 also binds to its own promoter in an apparent feed-forward mechanism (Mao et al., 2011). However, even with this well-studied TF, genetic analysis has indicated that WRKY33 targets multiple signaling pathways simultaneously, some of which are still unknown.

The recent analysis of WRKY33 function highlights the value of time series analyses (Birkenbihl et al., 2012). Transgenic *wrky33* knockout lines showed wild-type induction of JA responses up to 14 h after inoculation (HAI), but from 24 HAI, repression of these JA-responsive genes occurred in the mutants. However, most global analyses are static (i.e., a single time point) or include a small number of time points. Collection of time series data is a powerful approach to determine the overall process structure and the relative timing of modules of a response. Such data can also be used in mathematical approaches to predict interactions between modules and/or their components. High-resolution temporal analysis of host transcriptional reprogramming following pathogen infection, such as that presented here, is instrumental in identifying critical early defense responses, defining a temporal hierarchy of events and laying the foundations for reconstruction of gene regulatory networks incorporating feedback and crosstalk between modules in the network.

RESULTS

High-Resolution Time Series Expression Profiling Identifies 9838 Differentially Expressed *Arabidopsis* Genes Following *B. cinerea* Infection

Full genome expression profiles were obtained from *Arabidopsis* leaves following infection with *B. cinerea*, a fungal necrotroph. Leaf 7 was detached from 192 4-week-old *Arabidopsis* plants and either inoculated with a suspension of *B. cinerea* spores or mock inoculated. Over 48 HAI, expanding lesions developed on

the pathogen-inoculated leaves (Figure 1). Every 2 HAI (up to 48 HAI) four whole leaves were harvested from each treatment. Expression analysis was performed using CATMA (a complete *Arabidopsis* transcriptome microarray) arrays (Sclep et al., 2007), cDNA from single leaves, and a statistically designed loop design of hybridizations (see Supplemental Figure 1 online), leading to a high-resolution, highly replicated time series of expression profiles (24 time points separated by 2 h; four biological and an average of three technical replicates for each time point in each condition).

Expression values for each CATMA probe at each time point in each biological replicate were extracted using a mixed-model analysis in a locally adapted version of the R package MAANOVA (for microarray analysis of variance; Wu et al., 2003). This time series data set is longitudinal in that the data reflect the defense process over time, but also cross-sectional in that each sample was one leaf from a different plant (i.e., destructive sampling) so there is no particular connection between the individual biological replicates. Due to this hybrid nature of the data, we investigated three statistical tests for their ability to determine genes differentially expressed between mock-inoculated and *B. cinerea*–infected samples over time. A detailed description of this process is given in Methods. In brief, we combined the outputs of a standard F test within MAANOVA with that of a Gaussian process two-sample test (GP2S) (Stegle et al., 2010), based on the low false positive rates of these methods (see Supplemental Figure 2 online). We combined the top 10,600 gene probes ranked by GP2S with 236 additional gene probes identified by the F test. Probes that did not map to genes in the TAIR9 annotation and duplicate probes (two or more probes mapping to the same gene) were removed. Thus, the time series expression profiling identified 9838 *Arabidopsis* genes as differentially expressed between *B. cinerea*–infected and mock-inoculated leaves over time.

The expression profiles for each individual probe on the CATMA array can be viewed using a Web tool (under the "data" section at http://go.warwick.ac.uk/presta). This plots the expression profiles at all 24 time points for both the infected and mock-inoculated leaves. Variation in expression is shown as a bar representing one standard error. The full data set is available in the Gene Expression Omnibus (GEO) under accession number GSE29642.

As an initial validation of the data set, the profiles of genes previously identified as differentially expressed during *B. cinerea* infection (Mengiste et al., 2003; AbuQamar et al., 2006; Pré et al., 2008; Dhawan et al., 2009; Wang et al., 2009; Chen et al., 2010; Luo et al., 2010), and in several cases known to influence the progression of disease, were examined (see Supplemental Table 1 online). In the majority of cases (28/41), the genes were identified as differentially expressed in our time series and expression profiles matched that in the literature. In a further four cases, the genes were ranked below the GP2S cutoff, but manual inspection showed that they were differentially expressed and again the profiles matched those in the literature (see Supplemental Table 1 and Supplemental Figure 3A online). Three genes reported to be upregulated in the literature did not show differential expression in our time series (see Supplemental Figure 3B online). Intriguingly, six genes showed differential expression in the opposite direction in our study compared with the literature (see Supplemental Figure 3C online). These included two genes, *ANAC002/ATAF1* and *HUB1*, whose expression level influences defense against *B. cinerea* (Dhawan et al., 2009; Wang et al., 2009). Using RT-PCR, we tested expression of *ATAF1* and *LOX2* in RNA from two of the four

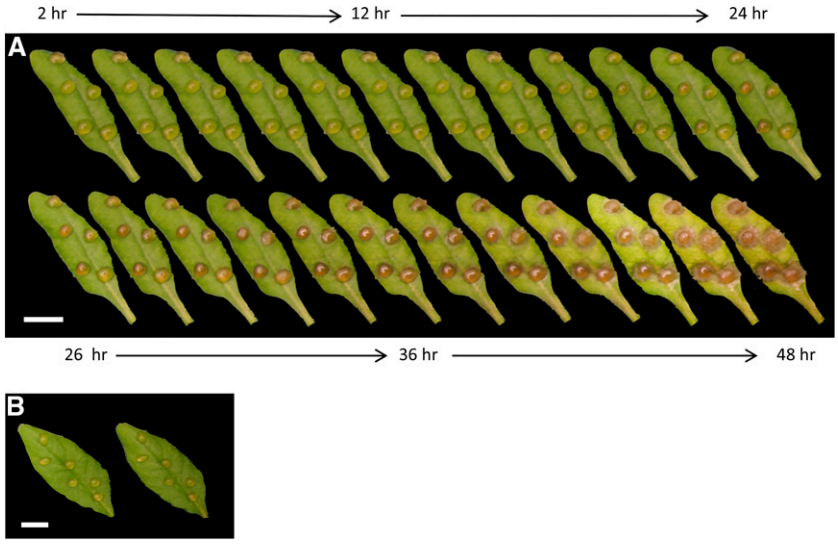

Figure 1. Time Series of *B. cinerea* Infection on *Arabidopsis* Leaf 7.

(A) Ten-microliter droplets of a suspension of *B. cinerea* spores (1×10^5 spores mL^{-1}) were placed on detached leaf 7 from 4-week-old *Arabidopsis* plants. Images show the same leaf every 2 h after inoculation until 48 h.
(B) A mock-inoculated leaf at 2 HAI (left) and 48 HAI (right).
Bars = 10 mm.

biological replicate samples at eight time points (see Supplemental Figure 3D online). The profiles matched those from the whole time series, indicating that the difference in expression was not due to the probes on the CATMA arrays; it seems that expression of even key genes varies depending on the environmental conditions, infection strategy, or isolate of *B. cinerea* being used.

Obviously, changes in transcription are not the only regulatory mechanism employed by plants to regulate their immune response. Our subsequent analysis of these differentially expressed genes (DEGs) and interpretation of such analyses is based solely on transcriptional events, although other regulatory mechanisms are possible.

The Time Series Expression Profiling Spans Multiple Stages of Infection

B. cinerea infection was initiated by pipetting droplets of spore suspension onto the top surface of detached leaves. The first visual symptoms of infection at 20 HAI are a darkening of the leaf surface under the inoculum droplets (Figure 1) and correspond to primary lesion formation following penetration of the host. Expansion of the lesion beyond the inoculum droplets is evident at 36 HAI and continues throughout the 48-h sampling period. We determined the expression of the *B. cinerea* β-tubulin gene relative to a nonchanging *Arabidopsis* gene (*PUX1*, *At3g27310*) as a measure of fungal growth (Figure 2). An initial rapid increase in tubulin expression/fungal biomass can be attributed to germination of conidiophores and hyphal growth in the inoculum media. A lag phase in growth is apparent between 20 and 28 HAI, during which time initial lesion formation occurs. Trypan blue staining of infected leaf tissue in the middle of the lag phase showed fungal hyphae as well as a claw arrangement of much thicker tubular structures (Figure 2B). These claw-like structures have been associated with penetration of the host and appear to develop from hyphae rather than undifferentiated germ tubes (Kunz et al., 2006). The lesion expansion stage appears to begin by 32 HAI with fungal biomass once again increasing and lesion expansion visible on the leaves from 36 HAI.

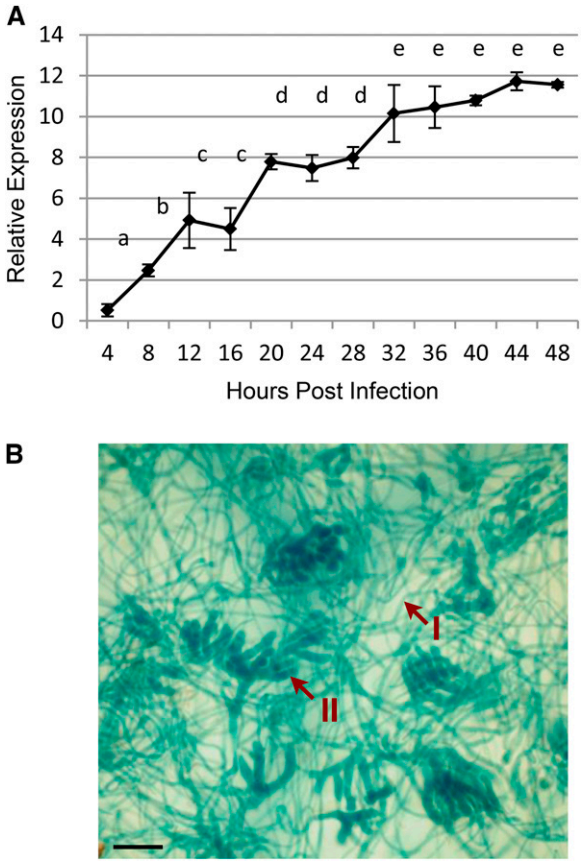

Figure 2. Growth of *B. cinerea* in *Arabidopsis* Leaves.

(A) Growth measured by expression of the *B. cinerea* tubulin gene. Expression levels were determined using real-time PCR and are shown as the $\log_2$ ratio of expression of *B. cinerea Tubulin* relative to *Arabidopsis PUX1* (*At3g27310*). Error bars indicate SE of three biological replicates. A one-way analysis of variance was performed to determine which pairs of adjacent time points differed significantly from each other. Significantly different groups ($P \leq 0.05$) are labeled a to e.

(B) Trypan blue staining of *Arabidopsis* leaves infected with *B. cinerea* 24 HAI. Red arrows: I, filamentous hyphae; II, large claw-like structures. Bar = 25 μm

Clustering of DEG Expression Profiles Reveals Coexpression of Functionally Related Genes

To look at the overall patterns in gene expression during the infection process, the 9838 DEGs were clustered using the SplineCluster algorithm (Heard et al., 2005) on the basis of their expression in infected leaves. Some of these DEGs show diurnal variation in expression in the mock-inoculated leaves (see the section "*B. cinerea* infection dampens clock gene oscillations" below); however, changes in response to infection override diurnal patterns, hence clustering on the basis of expression profile during infection is valid. Using a prior precision value of 0.001, 44 clusters were obtained that are shown in Figure 3 (two of which are singleton clusters). From a heat map of these 44 clusters, it is clear that a major shift in gene expression (up and down) of infected leaves occurs by ~26 HAI (see Supplemental Figure 4 online). This major transcriptome change occurs before visible lesion formation during the lag phase of *B. cinerea* growth (Figure 2). Despite this major change, clusters of genes whose expression changes earlier or later than this point in infection and clusters showing transient changes in expression are also visible. The list of genes in each cluster is given in Supplemental Data Set 1 online.

The 44 clusters represent groups of genes that are coexpressed over the time course of infection. We analyzed these groups for overrepresentation of Gene Ontology (GO) terms (Ashburner et al., 2000) using BiNGO (Maere et al., 2005) to ask whether genes in the same cluster are involved in the same biological process, suggesting coordinated regulation of the process. Many different terms were overrepresented in these clusters (see Supplemental Data Set 2 online), suggesting coregulation of genes and highlighting the breadth of the response to this pathogen.

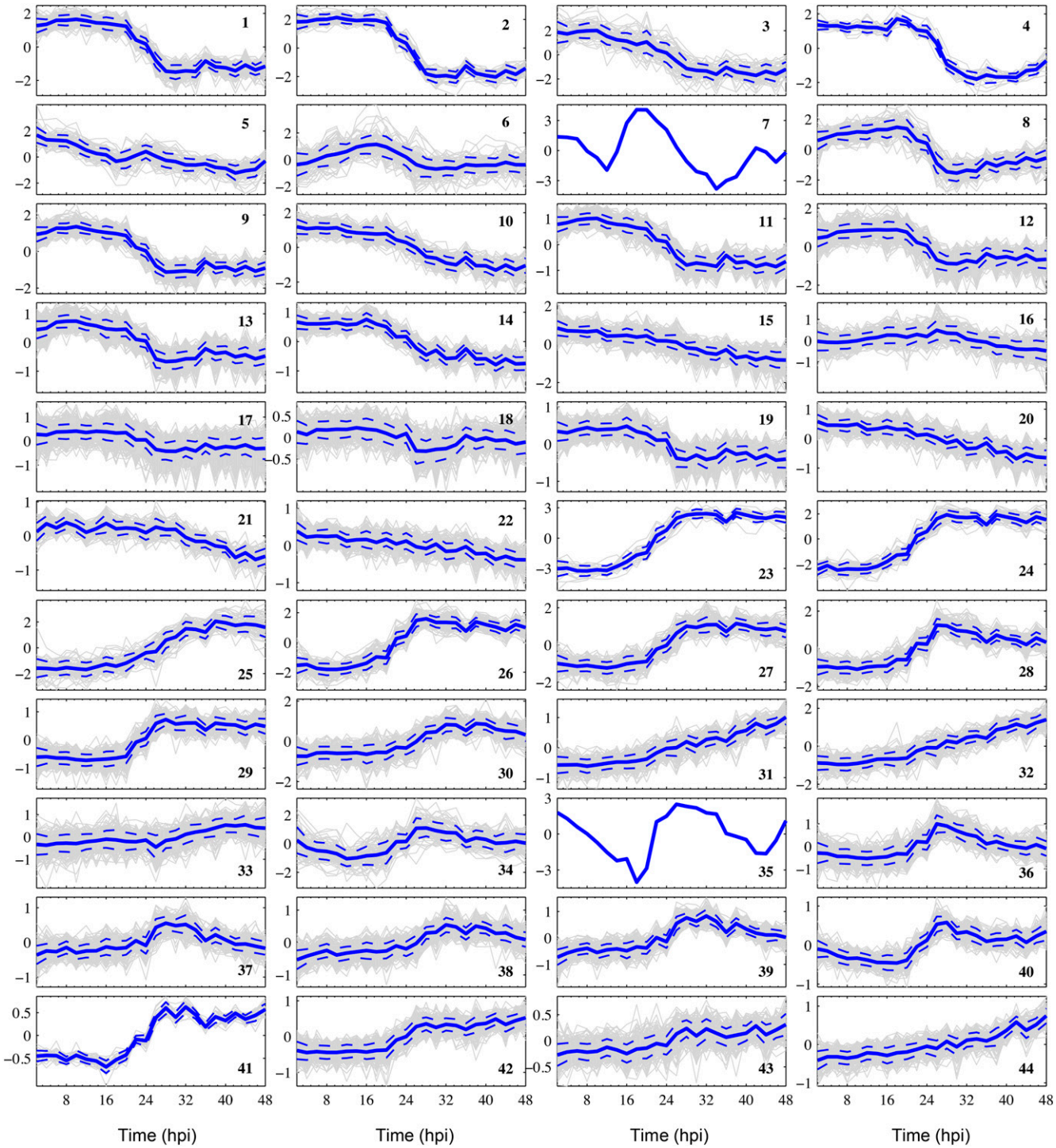

Figure 3. Infected Leaf Expression Profiles of the Gene Members of Each of the 44 Clusters Generated by SplineCluster.

The individual gene profiles are shown as gray lines with the mean profile in dark blue. The dashed blue lines indicate the mean ± 1 SD of the cluster. The *y* axes indicate $\log_2$ expression normalized on a per gene basis. hpi, hours post inoculation.

Chronology of the Defense Response

We specifically wanted to identify biological processes that were taking place during the early stages of *B. cinerea* infection, since these are more likely to influence the outcome of the plant–pathogen interaction and the chronology of the defense response. Two methods were used to investigate the timing of gene expression changes. First, a Gaussian process regression analysis was used to identify the time point at which there is a change in the rate of each gene's expression. A gradient significantly greater or less than zero indicates expression of the gene is increasing or decreasing, respectively; a gradient of zero indicates a steady level of expression. This analysis was described in detail by Breeze et al. (2011). From the gradient information for each gene, the first time at which at least half of the genes in a cluster have a significantly increasing or decreasing gradient was calculated. This gave a single time point for each cluster indicating the time at which expression of the genes in that cluster began to change following infection (see Supplemental Data Set 2 online) and enables us to chronologically order the biological processes identified through GO analysis of the SplineClusters (Figure 4).

SplineCluster groups genes on the basis of similarity of their expression profiles over time. We were also interested in whether genes could be grouped in a meaningful way using the time at which a gene is first differentially expressed after infection. A time-local version of the GP2S test (Stegle et al., 2010) was used to determine the time at which each of the 9838 DEGs was first differentially expressed in the *B. cinerea*–infected leaves compared with mock inoculated leaves. Seventy-four genes were not identified as differentially expressed using this model, but a time of first differential expression (TOFDE) was determined for the remaining 9764 genes. In the time-local GP2S, the 48-h time series was split into 100 increments; hence, TOFDE was calculated to the nearest half hour. TOFDE was used to group the DEGs in bins of 30 min, 1 h, or 2 h. These represent groups of genes that respond to *B. cinerea* infection of *Arabidopsis* leaves at the same time and were analyzed for

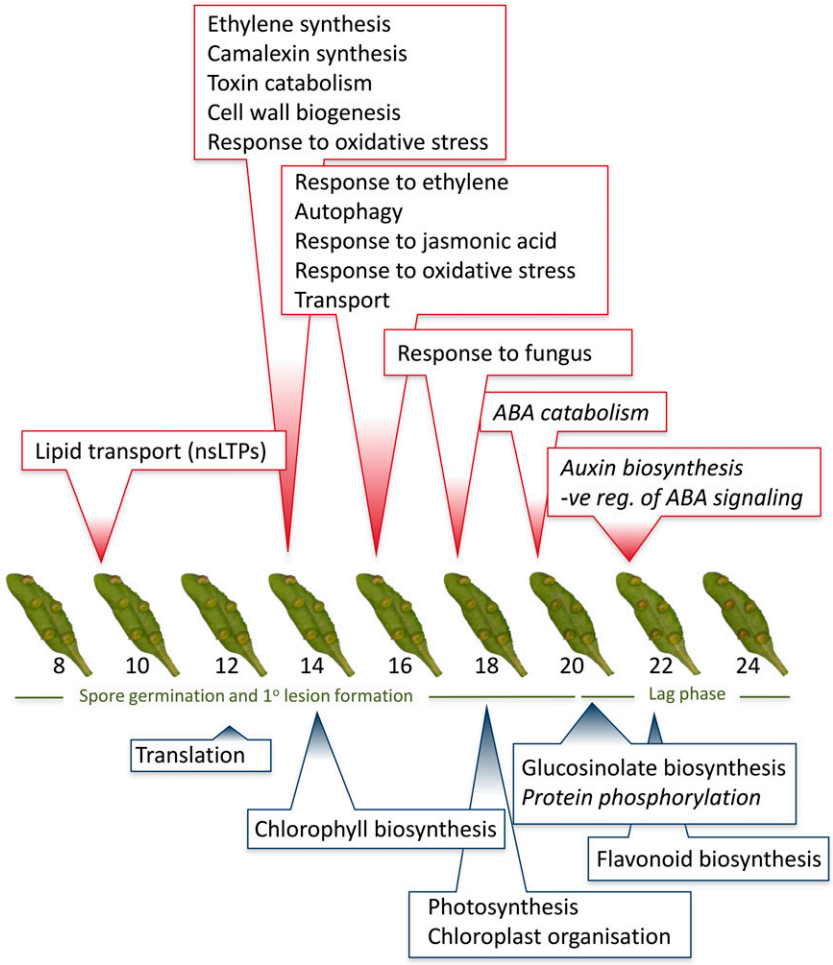

Figure 4. Selected GO Terms Overrepresented in Clusters of Genes Differentially Expressed after *B. cinerea* Infection of *Arabidopsis* Leaves.

GO terms are aligned with the time of gradient change and/or time of first differential expression of the cluster (in italics), with red boxes containing GO terms from upregulated genes and blue boxes containing GO terms from downregulated genes.

overrepresented GO terms again using BiNGO (Maere et al., 2005). GO terms overrepresented in specific time bins are listed in Supplemental Data Set 3 online with selected terms again highlighted in Figure 4. TOFDE does not separate genes differentially expressed around the middle of the time series as well as the gradient tool analysis; however, it did highlight some additional processes occurring during infection.

Signaling

Key events in many plant responses are the synthesis and/or response to phytohormones. The involvement of ET, auxin, abscisic acid (ABA), and JA was highlighted by overrepresented GO terms. *Arabidopsis* defense against necrotrophic pathogens, including *B. cinerea*, is known to involve or be affected by ET, auxin, ABA, and JA (Thomma et al., 1998, 1999; Audenaert et al., 2002; Pandey et al., 2005), but our analysis enables the order of synthesis and/or action of these hormones to be elucidated. At 14 HAI, two genes encoding 1-aminocyclopropane-1-carboxylate synthases (ACS2 and ACS6), enzymes catalyzing the first and rate-limiting step in ET biosynthesis, are upregulated. ACS2 and ACS6 proteins are known to be responsible for the majority of *B. cinerea*–induced ET production and are phosphorylated and stabilized by MPK3/6 (Han et al., 2010); however, genes encoding ACS enzymes are also known to be transcriptionally activated (Tsuchisaka and Theologis, 2004). Analysis of an *acs2 acs6* double mutant suggests that another ACS protein is also involved in ET production in response to *B. cinerea* infection (Han et al., 2010). However, although all nine *ACS* genes were on the CATMA arrays, only *ACS2* and *ACS6* are differentially regulated in our analysis. Synthesis of ET should lead to downstream events; hence, the overrepresentation of the GO term "response to ET" 2 h later and "ET-mediated signaling" highlighted in the time bins analysis. Genes responsible for these terms include *EBF2* with a known role in ET signaling (Saito et al., 2004) and two TFs from the ET response factor family, At *ERF15* and *ORA59*.

"Response to JA stimulus" is a GO term overrepresented in the same early cluster of genes responding to ET (16 HAI). Genes corresponding to this term include *ERF1* and *MYB108*, for which overexpressor and knockout lines, respectively, show altered *B. cinerea* susceptibility (Berrocal-Lobo et al., 2002; Mengiste et al., 2003), four genes with a known role in defense (*PROPEP1*, *ERF4*, *PEN1*, and *MYB51*) (Huffaker et al., 2006; Kwon et al., 2008; Pré et al., 2008; Clay et al., 2009), and *MYB13*, whose expression is induced by *B. cinerea* in a JA/ET-dependent manner (AbuQamar et al., 2006). The remaining gene, *VTC5*, has no known defense role, but its coexpression with these other defense regulators makes this a viable hypothesis. Interestingly, ERF4 mediates antagonism between the ET and ABA pathways with overexpression of *ERF4* leading to decreased sensitivity to ABA (Yang et al., 2005).

"Auxin biosynthesis" is overrepresented in genes upregulated 22 HAI. This group of genes includes anthranilate synthase (*ASA1*), a rate-limiting step in the synthesis of the auxin precursor Trp, *STY1*, a transcriptional activator of auxin biosynthesis (Eklund et al., 2010), and two paralogous genes (*RGLG1* and *2*) thought to be responsible for directional flow of auxin (Yin et al., 2007). At least in roots, *ASA1* and *ASB1* are required for ET-mediated increases in auxin (Stepanova et al., 2005). Hence, the earlier synthesis of ET we observe suggests that a similar mechanism is operating during response to *B. cinerea* infection; ET activates auxin biosynthesis via ASA1.

ABA-associated GO terms suggest a strong repression of ABA signaling during infection by *B. cinerea* (Figure 4). ABA catabolism is overrepresented in the group of genes first differentially expressed 20 HAI due to the upregulation of *CYP707A3* and *UGT71B6*. CYP707A3 catalyzes both 8′- and 9′-hydroxylation of ABA, with 8′-hydroxylation being the major pathway of ABA catabolism (Saito et al., 2004; Okamoto et al., 2011), while UGT71B6 glycosylates ABA to supposedly inactive conjugates (Priest et al., 2005). Two hours later (22 HAI) upregulation of negative regulators of ABA signaling begins. ABI1 and ABI2, two protein phosphatases involved in the core ABA pathway, are induced along with two repressors of ABA responses: ABR1, thought to be a transcriptional repressor (Pandey et al., 2005), and TMAC2, a nuclear-localized protein (Huang and Wu, 2007). AZF2 also has a TOFDE of 22 HAI and is another repressor of ABA signaling (Drechsel et al., 2010). Three of the genes encoding the soluble PYL/PYR/RCAR ABA receptors (*PYL8*, *PYL9*/*RCAR1*, and *PYR1*) are grouped in cluster 12 and begin to change in expression 18 HAI. All three genes are downregulated, lending weight to the hypothesis that ABA signaling is repressed during *B. cinerea* infection.

Plant hormones play a major role in defense, and this analysis has provided a timeline of the synthesis and/or action of these during infection. However, other signaling mechanisms are also highlighted by the GO term analysis of clusters. The term "lipid transport" is overrepresented in a cluster of genes that are upregulated very early after infection (10 HAI, cluster 6). Genes annotated with this term include two nonspecific lipid transfer proteins (nsLTPs), *LtpV.2* and *LtpV.3* (Boutrot et al., 2008), and the two xylogen proteins in *Arabidopsis*, *XYP1* and *XYP2*, which also contain a nsLTP domain (Motose et al., 2004). *XYP1* in particular responds early to *B. cinerea* infection, and all four genes are downregulated around 25 HAI. The physiological function of nsLTPs is not well understood, and only a few have been demonstrated to bind lipids. They are thought to have a defense function and as such have been characterized as pathogenesis-related protein family 14 (van Loon and van Strien, 1999). However, XYP1 and XYP2 have a role in vascular differentiation (Motose et al., 2004) and have not previously been implicated in plant defense. The coordinated expression of several nsLTP-containing proteins suggests they have a specific role in defense.

Crosstalk between signaling pathways mediating plant responses to biotic and abiotic stress is well known with a growing number of genes involved in these interactions being identified (Fujita et al., 2006). This crosstalk is also evident from our *B. cinerea* infection time series expression data. "Response to abiotic stress" and more specific child terms are overrepresented in several clusters of DEGs (Figure 5). These clusters include both up- and downregulated genes and span both the primary lesion formation and lag phases of infection. Gradient analysis gave clusters 5, 6, and 34 change times of 8, 10, and 6 HAI, respectively. However, the TOFDE for each of the genes annotated with an abiotic stress

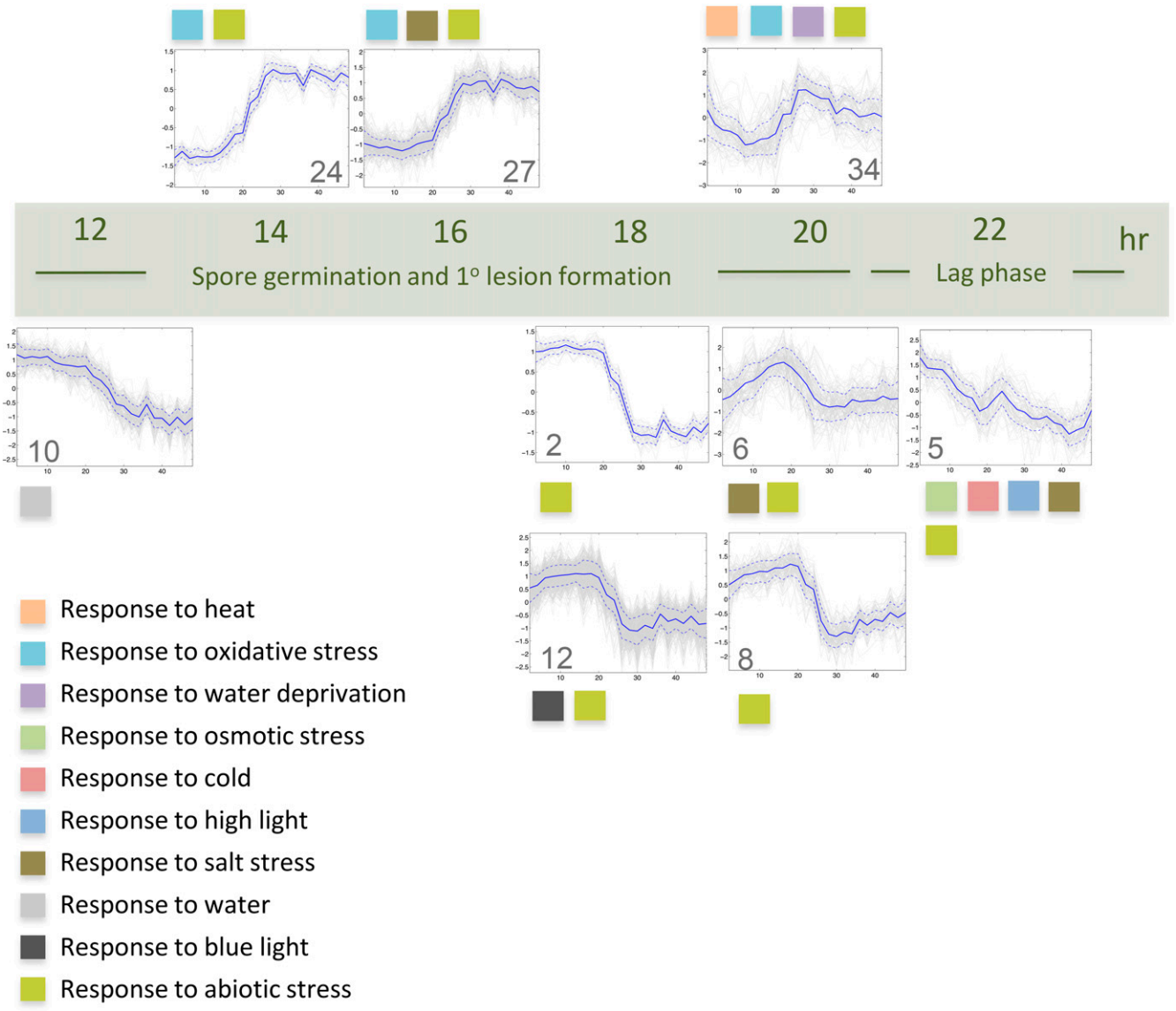

Figure 5. GO Terms Relating to Abiotic Stress Responses Overrepresented in Clusters of Genes Differentially Expressed after *B. cinerea* Infection of *Arabidopsis* Leaves.

GO terms are aligned with the time of gradient change and/or time of first differential expression of the cluster, with the cluster expression profile shown. All "response to abiotic stimulus" and nonredundant individual abiotic stress GO terms are shown.

GO term was much later, and manual inspection of the gene profiles indicated that the TOFDE values were correct; hence, this is the timing used in Figure 5. This discrepancy occurs because many of these genes show diurnal patterns of expression hence the mock expression profiles are also changing over time.

Metabolism

One of the most striking findings is the downregulation of photosynthesis and associated processes in response to infection. Downregulation of chlorophyll biosynthesis in comparison to the uninfected controls appears to start around 14 HAI but "chlorophyll biosynthesis" is also an overrepresented GO term in clusters whose expression begins to drop at 18 and 20 HAI (clusters 1, 2, and 8). The genes decreasing in expression encode many enzymes required for chlorophyll biosynthesis (such as HEME1, HEME2, and a subunit of Mg-chelatase) as well as GUN4, a regulatory protein that promotes chlorophyll biosynthesis by binding to Mg-chelatase (Adhikari et al., 2011). Chloroplast organization and biogenesis is also overrepresented in cluster 9, containing genes decreasing in expression at 18 HAI.

Photosynthesis is overrepresented in three clusters (1, 2, and 9) that show a drop in expression starting at 18 HAI. It is also

overrepresented in cluster 4, whose genes start to decrease in expression at 22 HAI. The genes annotated with this term in these clusters encode many components of photosystems I and II. The concerted downregulation of photosynthesis during biotic stress is a well-known phenomenon and has been seen in many very different plant biotic interactions (Bilgin et al., 2010). It has been suggested that the downregulation of photosynthetic gene expression enables the plant's nitrogen resources to be reallocated for synthesis of new defense proteins. The GO term "regulation of photosynthesis" is overrepresented in cluster 12, whose genes start to drop in expression at 18 HAI. Three genes are annotated with this term: *STN7*, *STN8*, and *DGD1*. STN7 is required for state transitions to balance absorbed light energy between the two photosystems (Bellafiore et al., 2005), and STN8 is required for phosphorylation of core photosystem II proteins. However, both of these kinases also regulate photosynthetic gene expression, and expression of three of the genes highlighted by our GO analysis is dependent on STN7 and STN8 function (Bonardi et al., 2005). Hence, even in our high-resolution time series, we appear to find the expression profiles of regulators and their targets clustering together.

Genes encoding enzymes of specific secondary metabolic pathways are also changing in expression during infection. One of the early changes (14 HAI) is highlighted by the overrepresentation of the GO term "indolalkylamine metabolic process" in cluster 26, due to the presence of two genes of the camalexin synthesis pathway, *CYP79B2* and *TSB2*. *TSB2* encodes the Trp synthase β-subunit converting 3-indoylglycerol phosphate to Trp, and *CYP79B2* encodes an enzyme responsible for conversion of Trp into indol-3-ylacetaldoxime, a metabolic step common to both camalexin and indole glucosinolate biosynthesis. Three cytochrome P450 enzymes (CYP71A15, CYP71A13, and CYP71B15) catalyze reactions specific to camalexin biosynthesis; however, these are not present on the CATMA arrays. The accumulation of camalexin during biotic stress is a well-known phenomenon, and camalexin levels are inversely correlated with susceptibility of *Arabidopsis* to *B. cinerea* infection (Denby et al., 2004). Trp can also be converted via tryptamine to strictosidine, an alkaloid. Three genes encoding strictosidine synthases are downregulated at 18 HAI, perhaps helping target indolic groups preferentially to camalexin synthesis.

Levels of indolic and aliphatic glucosinolates as well as flavonols have been shown to decrease around a developing *B. cinerea* lesion (Kliebenstein et al., 2005), and this analysis indicates this occurs after activation of camalexin synthesis. A group of genes involved in flavonoid biosynthesis is downregulated around 22 HAI. These genes (*At3g51240*, flavanone 3-hydroxylase; *At4g22880*, leucoanthocyanidin dioxygenase; and *At5g05270*, chalcone-flavanone isomerase) are also clustered with genes encoding sinapoylglucose1 and 4-coumarate-CoA ligase3, indicating downregulation of the more extensive phenylpropanoid pathway at this time. The genes are grouped in cluster 6 (judged by the gradient tool to increase in expression 10 HAI); however, inspection of the infected and mock expression profiles for these genes indicates that they are only differentially downregulated at 22 HAI. The term "glucosinolate biosynthesis" is overrepresented in a cluster downregulated at 20 HAI. This cluster contains several genes involved in the synthesis of aliphatic glucosinolates (*BCAT4*, *MAM1*, *CYP83A1*, and *CYP79F2*) as well as a key regulator of this pathway, *MYB28* (Sønderby et al., 2007). *MYB29*, another regulator of aliphatic glucosinolates (Sønderby et al., 2007), is also downregulated at the same time during infection but clusters separately.

The cell wall is known to play a key role in pathogen defense both structurally and in a signaling capacity (Cantu et al., 2008; Hématy et al., 2009), although the exact mechanisms of cell wall signaling are just beginning to be elucidated. In our time series data, two clusters of genes are overrepresented for GO terms associated with the cell wall and are differentially expressed relatively early after infection. Cluster 11 contains two cellulose synthase genes, *CeSA1* and *CeSA3*, both with roles in defense signaling. The *cev1* mutation of *CeSA3* has decreased susceptibility to *B. cinerea*, most likely due to overproduction of JA and ET and associated downstream gene expression (Ellis et al., 2002). The *rsw1* mutant of *CeSA1* also exhibits increased expression of *VSP1*, suggesting overproduction of JA in this mutant as well. Consistent with reduction in activity of these genes leading to activation of defense signaling, CeSA1 and CeSA3 are downregulated during *B. cinerea* infection. Knockouts of a secondary cell wall regulator, *MYB46*, were recently shown to be less susceptible to *B. cinerea* (Ramírez et al., 2011a). Downregulation of six cellulase synthase genes (including *CeSA1* and *CeSA3*) following *B. cinerea* infection occurs more rapidly and to a greater degree in *myb46* knockout lines compared with the wild type (Ramírez et al., 2011b), suggesting the timing of CeSA repression may be crucial. Cluster 24 contains three cell wall–associated genes: a peptidoglycan binding protein containing a LysM domain (*At5g62150*), a predicted chitinase (*At2g43590*), and a member of the pectin methylesterase inhibitor (PMEI) superfamily (*At2g45220*). All these genes are strongly upregulated around 14 HAI and from their predicted functions are likely to have direct roles in combating *B. cinerea* within the cell wall environment. Chitin is a characteristic component of fungal cell walls; the LysM domain is thought to mediate binding to peptidoglycans and chitins, whereas chitinases can degrade chitin. PMEIs inhibit pectin methylesterases, maintaining a high level of methylated pectin in the cell wall, making the wall more resistant to degradation by enzymes, such as endopolygalacturonases, produced by pathogens. Overexpression of two characterized *Arabidopsis* PMEIs has been shown to confer decreased susceptibility to *B. cinerea* (Lionetti et al., 2007).

The ability to kill plant cells is vital to successful infection by *B. cinerea*. Recent genome analysis has indicated that *B. cinerea* has the ability to produce ~40 different toxins, including botrydial and botcinic acid, which have been previously characterized (Amselem et al., 2011). Not surprisingly, toxin catabolism is a functional GO term highlighted in our time series expression data. Seven glutathione *S*-transferase (GST) genes are present in two clusters (26 and 30) overrepresented for this term and are upregulated around 14 HAI. All seven genes (*GSTU3*, *GSTU7*, *GSTU8*, *GSTU10*, *GSTU19*, *GSTU24*, and *GSTU25*) are members of the Tau family of GSTs, which are plant specific and can bind glutathione conjugated fatty acid derivatives (Dixon and Edwards, 2009). Although the precise function of these GSTs is not known, GSTU19 and GSTU25 both have high conjugating activity toward the xenobiotic 1-chloro-2,4-dinitrobenzene, used

as an indicator of detoxifying activity. However, GSTU19 can conjugate glutathione onto oxylipins, suggesting that it may play a role in modulating jasmonate signaling (Dixon and Edwards, 2009). In addition to toxin detoxification, cells are able to prevent toxin accumulation through sequestration in the vacuole or active transport out of cells. The GO term "transport" is overrepresented in cluster 27, whose gene members are upregulated around 16 HAI. Three genes encoding MATE (multidrug and toxic compound extrusion) transporters (*AT1G66760*, *AT1G71140*, and *AT2G04100*) are in this cluster. Plant MATE proteins appear to transport a variety of secondary metabolites as well as xenobiotics (Omote et al., 2006), and two (EDS5 and ADS1) have been shown to positively and negatively regulate SA-mediated defense against biotic pathogens (Nawrath et al., 2002; Sun et al., 2011).

One of the first responses to infection highlighted in our study is the dramatic downregulation of components of the translational machinery. Seventy-four genes encoding ribosomal proteins are downregulated in three waves at 12, 18, and 28 HAI. Eighteen other genes encode translation initiation, elongation, and release factors as well as tRNA synthetases. Whether this global change is an active process mediated by the plant or an effect of pathogen-derived toxins is not clear, but the early change in expression of these components and the fact that their downregulation appears coordinated would suggest a specific function in the defense response.

Developmental Processes

Cluster 27 is overrepresented for the GO term "autophagy" due to four genes (*ATG8a*, *ATG8b*, *ATG7*, and *ATG18a*) all upregulated around 16 HAI. At first glance, the upregulation of autophagy genes suggests manipulation by the pathogen to enhance infection. However, a recent reverse genetics study has demonstrated that autophagy plays a positive role in defense against *B. cinerea* (Lai et al., 2011), and knockout mutants of *ATG7* and *ATG18a* exhibit increased susceptibility to this pathogen. The relatively early induction of these genes may be an indication of a genuine plant response rather than active manipulation by the pathogen.

The ability to group genes according to their TOFDE or expression profile during *B. cinerea* infection has identified coordinated changes in gene expression, indicating the early involvement of specific processes and the relative order of plant responses.

Comparison of Gene Expression Patterns during *B. cinerea* Infection and Developmental Leaf Senescence Shows Considerable Overlap but Reveals Specific Features

Previous work has analyzed a similar time series of gene expression changes during leaf senescence in *Arabidopsis* and identified over 6000 genes showing differential expression over the 22 d from leaf expansion to senescence (Breeze et al., 2011). These data provide an exciting opportunity to compare and contrast gene expression changes between senescence and defense against *B. cinerea* infection. The two plant responses are very different in timing but may involve similar signaling pathways. Lists of gene differentially expressed in each treatment were divided into up- or downregulated genes. For the senescence data from Breeze et al. (2011), clusters 1 to 24 were classed as downregulated and clusters 27 to 48 as upregulated, with genes in clusters 25 and 26 being omitted from the analysis due to them showing both up- and downregulation. For genes differentially expressed in response to *B. cinerea* infection, clusters 23 to 44 were classed as upregulated and clusters 1 to 22 as downregulated.

Overlapping genes in the four lists (*B. cinerea* up/down and senescence up/down) were identified. A total of 3759 genes showed differential expression in both data sets; however, the vast majority of genes (8126) were specifically differentially expressed under one condition only (Figure 6). In most cases, genes differentially expressed during both senescence and *B. cinerea* infection were similarly regulated in each response: 1405 genes upregulated and 1767 downregulated. However, 502 genes were upregulated during senescence but downregulated following *B. cinerea* infection, while only a small group showed the opposite profile (85 genes). Genes in all eight groups are listed in Supplemental Data Set 4 online.

GO term analysis was applied to each set of genes to identify pathways and functions common or specific to the two responses. Selected overrepresented terms for each group of genes are shown in Figure 6 with the full set listed in Supplemental Data Set 5 online. As expected, very high over representation of genes involved in photosynthesis, chlorophyll biosynthesis, and starch metabolism was observed in the downregulated genes common to both processes. Genes responsive to ABA, ET, JA, and SA are all overrepresented in genes upregulated in both senescence and *B. cinerea* infection, highlighting the important role plant hormones play in both of these stress responses. However, there are still condition-specific aspects of hormone involvement indicating complex differential activation in the two processes. Different groups of ABA-responsive genes are upregulated during senescence and *B. cinerea* infection, upregulated in senescence only, and upregulated in senescence but downregulated during *B. cinerea* infection. Similarly, ET-responsive genes are overrepresented in both the senescence and *B. cinerea* upregulated group and *B. cinerea* infection only, while different SA-responsive genes are upregulated in both conditions as well as downregulated during *B. cinerea* infection only. Markedly, the involvement of cytokinin and brassinosteroid hormones appears specific to senescence. The specific downregulation of several *Arabidopsis* response regulator genes and cytokinin response factors during senescence, and not during *B. cinerea* infection, suggests that the repression of the photosynthetic machinery that occurs during both senescence and infection is not dependent on changes in cytokinin levels.

The aromatic amino acid biosynthesis pathway appears to be important only during *B. cinerea* infection, and genes encoding enzymes involved in phenylpropanoid, chorismate, Trp, Tyr, and Phe biosynthesis are all upregulated. One of the roles of the Trp pathway during pathogen infection is to provide substrate for camalexin synthesis. The antimicrobial activity of camalexin is clearly not relevant to the senescence process. Upregulation of genes involved in glutathione metabolism also appears specific to *B. cinerea* infection. Genes encoding glutathione biosynthetic enzymes as well as GSTs and enzymes involved in the reduction of oxidized glutathione and degradation of glutathione conjugates

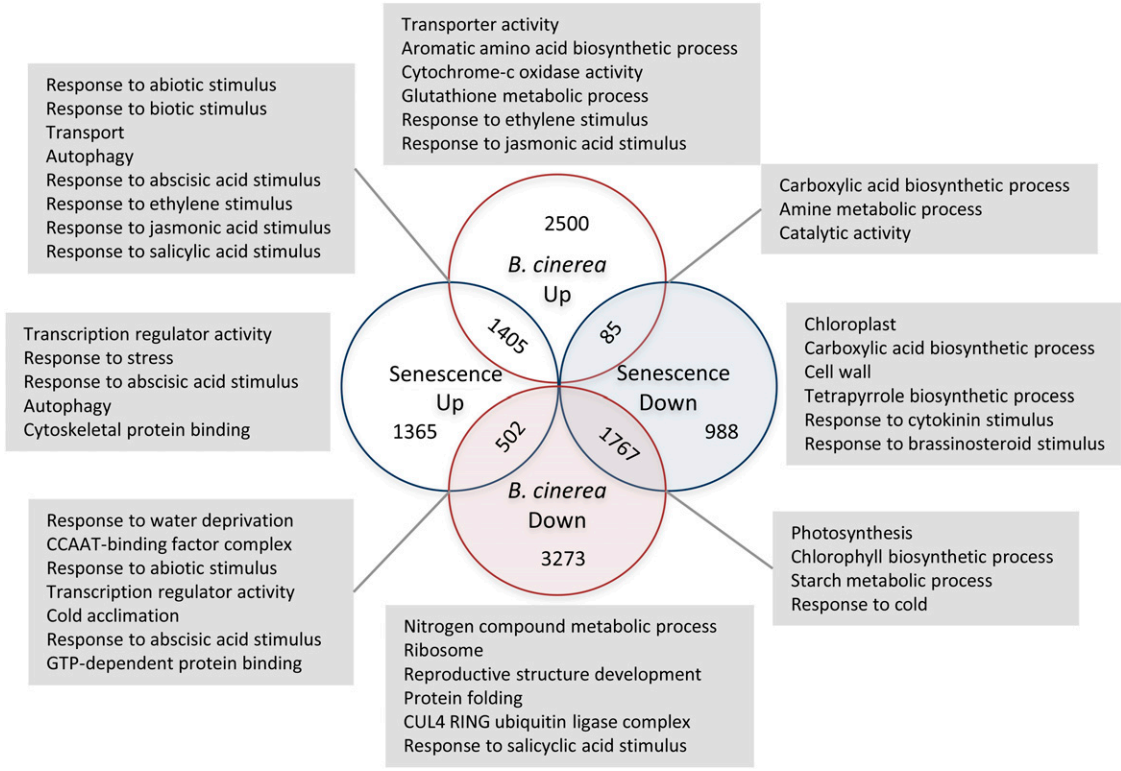

Figure 6. Number and Function of Genes Differentially Expressed during Both Natural Senescence and *B. cinerea* Infection.

The number of genes up- and downregulated during senescence and *B. cinerea* infection and overlaps between these is shown in the Venn diagram. Selected overrepresented GO terms are shown for each subset of genes.
[See online article for color version of this figure.]

are only upregulated during pathogen infection. This may well reflect the increased burden of oxidative stress that the plant has to cope with during *B. cinerea* infection, as well as the presence of many toxins. It may also reflect the demand for camalexin, which uses glutathione in its production.

Despite the common involvement of several plant hormones, many genes involved in the regulation of transcription are induced during senescence only or differentially expressed during senescence (up) and *B. cinerea* infection (down). The NF-Y TF family (corresponding to the CCAAT binding factor complex) is clearly regulated very differently in the two responses. In mammals, a heterotrimeric complex of NF-YA, NF-YB, and NF-YC subunits is required for DNA binding of these TFs to the CCAAT motif. Of the 36 NF-Y genes in *Arabidopsis*, 26 are differentially expressed during senescence and/or *B. cinerea* infection. Only one gene, *NF-YB4*, is similarly expressed (downregulated) during both conditions. The remaining 25 genes are differentially regulated during senescence and *B. cinerea* infection; six are upregulated and one downregulated in only senescence, nine upregulated and two downregulated in just *B. cinerea* infection, and seven upregulated in senescence and downregulated in pathogen infection. This family of TFs therefore appears to be key determinants of regulatory specificity in these stress responses. Another level of specificity is also apparent; many NF-YA subunits show increased expression during senescence, while NF-YB and NF-YC subunits are upregulated following *B. cinerea* infection.

B. cinerea Infection Dampens Clock Gene Oscillations

There has been much circumstantial evidence about the influence of the circadian clock on pathogen defense (Roden and Ingle, 2009). However, a small polypeptide PCC1, whose overexpression leads to resistance against *Hyaloperonospora arabidopsidis*, is under both defense and circadian regulation (Sauerbrunn and Schlaich, 2004), and, recently, a group of genes involved in basal and *R*-mediated defense was shown to be under the control of CCA1, a core clock component (Wang et al., 2011). In the latter study, the central clock oscillator appeared unaffected by *H. arabidopsidis* infection. By contrast, *B. cinerea* infection of *Arabidopsis* leaves appears to influence expression of core clock genes, suggesting a stress input into the central oscillator. The timing of core clock gene expression is not perturbed, but the amplitude of cyclical expression is reduced (Figure 7). The reduction in amplitude affects genes expressed at different phases of the clock and appears to start around 24 HAI.

In the mock-inoculated gene expression data, we identified 2404 genes that were expressed in a rhythmic fashion with an ~24-h period (see Supplemental Data Set 6 online). GO analysis

of these genes indicated that, as expected, the annotation "circadian rhythm" was significantly overrepresented. "Response to stress," "response to abiotic stress," and several terms associated with plant stress responses (for example, "response to cold," "response to ABA stimulus," and "response to reactive oxygen species") were also overrepresented in these rhythmic genes (see Supplemental Data Set 7 online). This is consistent with previous reports (Covington et al., 2008). When these 2404 genes were grouped according to their phase of rhythmic gene expression (using 2-h intervals), the GO term "response to abiotic stimulus" was significantly overrepresented in genes peaking in expression 8 to 12 h after dawn. Genes peaking in expression 10 to 12 h after dawn were overrepresented for several defense-related terms, including "JA biosynthesis," "response to fungus," and "response to biotic stress" (see Supplemental Data Set 8 online). Hence, in contrast with the CCA1-controlled defense genes identified by Wang et al. (2011), defense-related genes appear to peak in the early afternoon in our experiment. Over 60% of the 2404 rhythmic genes from the mock-inoculated leaves were differentially expressed in response to *B. cinerea* infection (1521 genes). In the vast majority of these cases (1407 genes), expression in response to infection overrode rhythmic expression, and these genes were not classified as rhythmic (with a period between 20 and 28 h) in the expression data from infected leaves.

Specific TF Binding Motifs Are Enriched in Groups of Coexpressed Genes

Clustering of DEGs based on their expression profile during *B. cinerea* infection groups coexpressed genes together and as seen above clearly enables specific processes in defense to be delineated. To ask whether this clustering can also identify coregulated genes, we analyzed the frequency of known TF binding motifs in the promoters of genes in each cluster. Despite the large number of DEGs, many clusters were enriched for specific TF binding motifs (Figure 8; see Supplemental Data Set 9 online). Furthermore, clusters with similar expression profiles are specifically enriched for similar motifs, with a clear difference between the motifs enriched in downregulated (1 to 22) and upregulated (23 to 44) clusters.

Clusters of genes that are suddenly downregulated ~20 HAI and associated with GO terms related to photosynthesis are enriched for variants of the G-box and I-box motifs, which have been shown to function in light regulated gene expression (Donald and Cashmore, 1990; Menkens et al., 1995). The apparently concerted

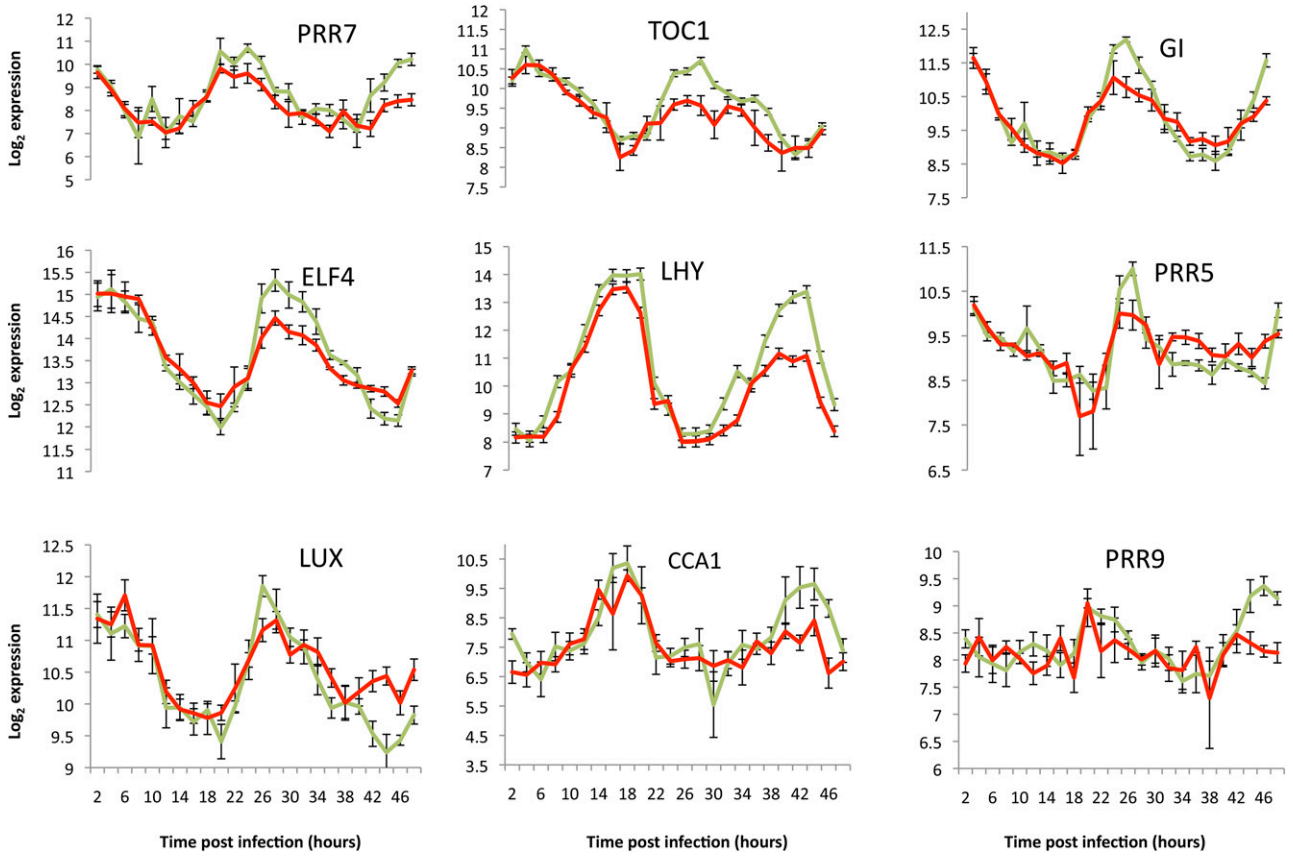

Figure 7. *B. cinerea* Infection Dampens Oscillations of Clock Gene Expression.

The green line indicates the mean expression profile of four biological replicates of mock-inoculated leaves, while the red line indicates the mean expression profile of four biological replicates of infected leaves. Error bars indicate SE (n = 4).

downregulation of such a large number of genes suggests repression of photosynthetic genes is highly coordinated. The G-box motif has been shown to interact with TFs that act as repressors, suggesting that downregulation of photosynthetic genes could be mediated through these motifs. For example, phytochrome interacting factors bind to the G-box motif present in the promoters of some photosynthetic genes (Huq and Quail, 2002; Huq et al., 2004), and some phytochrome interacting factors, such as PIF3 (Shin et al., 2009) and PIF7 (Kidokoro et al., 2009), have been shown to negatively regulate expression of photosynthetic genes. However, both *PIF3* and *PIF7* are downregulated during *B. cinerea* infection, suggesting other TFs are playing this role.

Many of the downregulated clusters are enriched for the site-II motif [TGGGC(C/T)], which serves as a binding site for TCP TFs (Martín-Trillo and Cubas, 2010). In addition to this site-II motif, consensus sequence motifs for both Class I and Class II TCP TFs were found enriched in these specific clusters. TCP proteins are commonly known as regulators of cell proliferation, growth, and development (Li et al., 2005; Hervé et al., 2009; Aggarwal et al., 2011; Kieffer et al., 2011). It is possible that developmental processes may be repressed as part of the defense response to direct resources toward fighting infection. However, three upregulated clusters are also enriched for TCP binding motifs, and TCPs also play a role in the circadian clock (Pruneda-Paz et al., 2009; Giraud et al., 2010) and control of JA biosynthesis (Schommer et al., 2008). Recently, TCP binding sites were shown to be enriched in calcium-responsive gene promoters (Whalley et al., 2011), which may explain the large number of defense-related gene promoters containing TCP binding motifs.

Dof family TFs interact with motifs that are enriched within both down- and upregulated clusters. Dof TFs, of which several are differentially expressed following infection, act as transcriptional activators or repressors in a wide range of biological processes (Yanagisawa, 2004), although as for the TCPs, these mostly include growth and developmental processes. However, expression of a group of three Dof TFs (OBP1-3) is induced by auxin and SA, and the majority of genes differentially expressed in a transgenic line overexpressing *OBP2* (Dof1.1) are involved in response to biotic stress (Skirycz et al., 2006). In particular, OBP2 regulates expression of several genes involved in indolic glucosinolate biosynthesis. Although these genes are also involved in the biosynthesis of camalexin and are induced in response to *B. cinerea* infection, *OBP1-3* are not differentially expressed in response to infection. This suggests additional members of the Dof family also play a role in biotic stress.

Members of the WRKY TF family are known to be involved in regulation of plant defense responses as both positive and negative regulators (Eulgem and Somssich, 2007). The W-box motif, which is bound selectively by members of the WRKY TF family, is overrepresented in clusters of genes rapidly induced 18 to 24 HAI (Figure 8). W-boxes are known to be enriched within the promoters of genes induced by biotic stress, and many WRKY TFs have a demonstrated function in defense against *B. cinerea* and other pathogens (for example, WRKY3, 4, 46, 53, and 70; Lai et al., 2008; Hu et al., 2012). WRKY TFs are overrepresented in TFs upregulated at many time points following *B. cinerea* infection (Figure 9). Despite this, W-boxes are enriched in specific clusters with a similar expression pattern.

Fifty-three AP2/EREBP TFs are differentially expressed following *B. cinerea* infection; however, the GCC-box, which is bound by AP2/EREBP TFs, is only overrepresented in cluster 22. This could indicate that multiple AP2/EREBP TFs operate at different times during infection, mediating different target gene expression patterns, or that alternative motifs can be bound by these TFs. A MYB TF binding motif is enriched within the promoters of genes in cluster 26 that are upregulated in response to infection. The motif was identified as the binding site for MYB80; however, neither *MYB80* nor the six other MYBs most closely related to *MYB80* are differentially expressed after *B. cinerea* infection, suggesting other MYB TFs may be involved. Several members of the MYB family have regulatory roles in response to biotic stress (Mengiste et al., 2003; Clay et al., 2009; Ramírez et al., 2011a), and 36 of the 132 MYB TFs in *Arabidopsis* (Stracke et al., 2001) are differentially expressed in response to *B. cinerea* infection.

NAC TFs are heavily linked with the regulation of abiotic stress responses (Nakashima et al., 2012). However, recent studies have indicated that this family of TFs also plays crucial roles in the response to biotic stress. Transgenic lines with reduced or increased expression of *ANAC002*, *ANAC019*, *ANAC055*, *ANAC081*, and *ANAC092* have altered susceptibility to pathogen infection (Delessert et al., 2005; Bu et al., 2008; Carviel et al., 2009; Wang et al., 2009; Wu et al., 2009) and all are differentially expressed following *B. cinerea* infection. Binding sites for NAC TFs are significantly overrepresented in a cluster of genes induced between 18 and 24 HAI with additional enrichment in clusters with similar expression profiles. The pattern of enrichment is consistent with the upregulation of many members of the NAC family around this time (Figure 9).

The evening element (Harmer et al., 2000) is overrepresented in two clusters of DEGs: one downregulated cluster (5) and one upregulated cluster (26) (see Supplemental Data Set 9 online). This element is required for evening-phased circadian regulation (Harmer and Kay, 2005) but has also been shown to play a role in the regulation of cold response genes (Mikkelsen and Thomashow, 2009). Intriguingly, 63 out of the 74 genes in cluster 5 are rhythmically expressed in mock-inoculated leaves, compared with only nine out of 134 genes in cluster 26. Perhaps cluster 5 represents the clock role of the evening element, while its overrepresentation in cluster 26 is indicative of a role in regulation of genes in response to infection.

Specific Families of TFs Are Differentially Expressed at Varying Times during *B. cinerea* Infection

From the TF binding motifs overrepresented in specific clusters of coexpressed genes, we obtain a pattern of TF activity. To investigate this further, we tested whether specific TF families were differentially expressed at coordinated times during the onset of infection. Using the GP2S time-local model, the times at which a gene is differentially expressed can be probabilistically identified. Using a specific threshold of $P \geq 0.5$, a binary time series model for each mRNA transcript was obtained indicating whether the transcript is differentially expressed (1) or not (0) at a given time. Using these models, and family-specific gene groupings, we identified a number of TF families that were

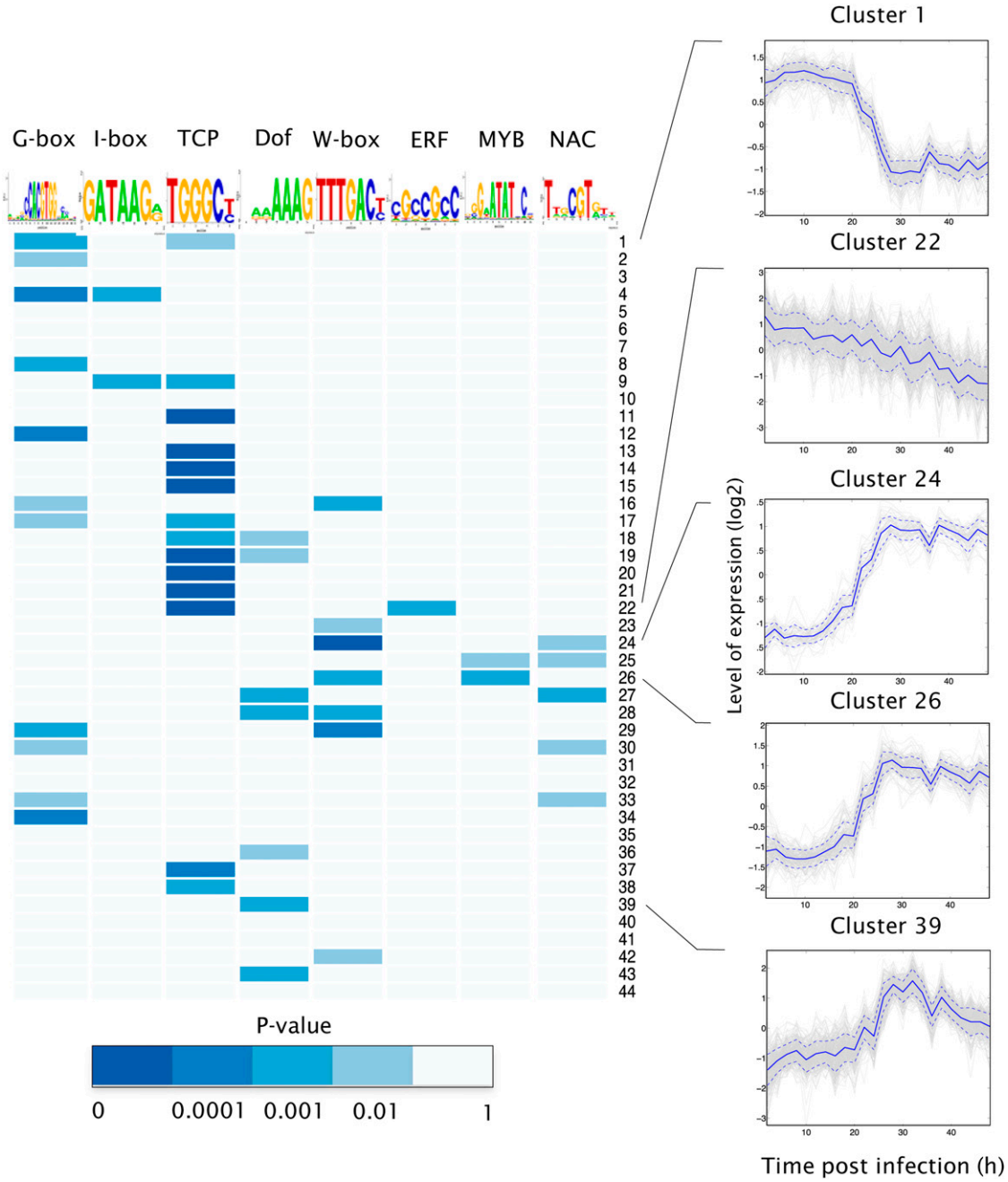

Figure 8. Known *cis*-Regulatory Sequences Associate with Groups of Coexpressed Genes.

Regulatory motifs (represented by sequence logos where character size indicates nucleotide frequency) are differentially enriched in the promoters of genes clustered on the basis of their expression during *B. cinerea* infection. The blue shaded boxes correspond to raw P value. Expression profiles from selected gene clusters that are enriched for TF binding motifs are shown on the right. Full results used to derive this figure are shown in Supplemental Table 9 online.

significantly overrepresented for DEGs at each time point during infection. Heat maps indicating the significance of each family's overrepresentation are shown in Figure 9 (separated into up- and downregulated). Numeric data are in Supplemental Data Set 10 online.

A number of TF families were significantly overrepresented for upregulated genes (adjusted $P < 0.05$), indicating significant coordinated transcriptional activity. The earliest highly significant overrepresentation is the WRKY family, around 18 HAI. Consistent with coordinated expression of this gene family, numerous regulatory interactions between WRKY TFs have been elucidated (Eulgem and Somssich, 2007; Pandey and Somssich, 2009). Furthermore, the coordinated upregulation of WRKY TFs from 18 HAI matches the overrepresentation of

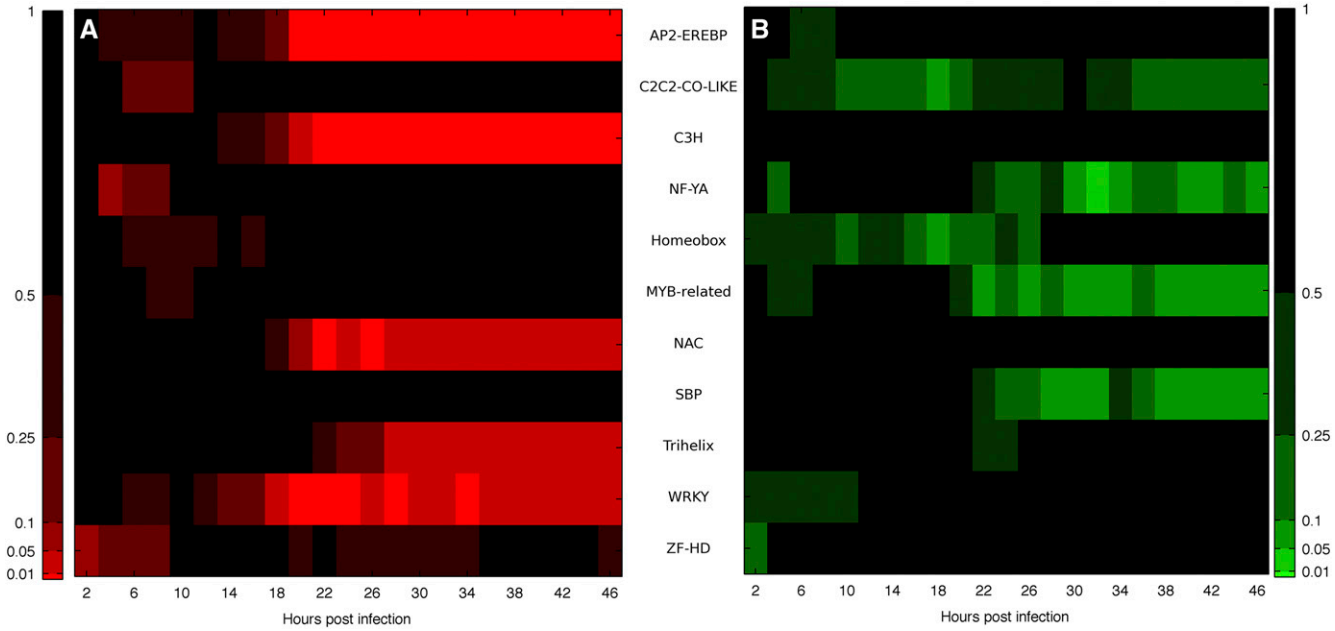

Figure 9. TF Families Significantly Overrepresented for DEGs, Indicating Distinct Periods of Regulation.

The plots show a number of TF families significantly upregulated (**[A]**, red) and downregulated (**[B]**, green) following *B. cinerea* infection. Color bars indicate P values (after FDR correction; Benjamini and Hochberg, 1995) with a range of significance thresholds (0.01, 0.05, 0.1, 0.25, and 0.5).

W-box motifs in clusters of genes differentially expressed over this period. Shortly afterwards, the NAC family is significantly upregulated, with the timing again matching the expression profiles of clusters enriched for NAC binding motifs. The AP2/EREBP TF family is significantly upregulated at the same time and contains many genes induced by hormones and/or biotic stress (Gutterson and Reuber, 2004). As indicated above, surprisingly, the binding motif associated with this family is only enriched in one downregulated cluster. Another large TF family, C3H, shows significant overrepresentation for upregulated genes. The proteins encoded by genes in this family possess a RING-type zinc finger domain, but the family structure, membership, and function are relatively uncharacterized. Significant coordinated expression during *B. cinerea* infection suggests this family may be involved in plant defense responses. Coordinated expression of Trihelix TFs is a later response to infection, from 28 HAI. This family (30 members in *Arabidopsis*; Kaplan-Levy et al., 2012) includes GT factors that bind to GT-boxes and repress light-inducible genes. However, as with the NAC family, the function of this family is expanding to include regulation of growth and abiotic/biotic stress responses. The WRKY, NAC, AP2-EREBP, and C3H families are also overrepresented in upregulated genes during senescence (Breeze et al., 2011), suggesting interconnected roles of these TFs in response to *B. cinerea* and senescence.

The only TF family showing significant coordinated downregulation is the NF-YA family at 32 HAI. This family contains genes encoding A subunits of the heterotrimeric NF-Y TF complex (a trimer of A, B, and C subunits). Individual NF-Y subunits have been shown to regulate several developmental processes and tolerance to abiotic stress (for example, embryo development and flowering time; Lee et al., 2003; Wenkel et al., 2006); however, a functional trimer has only been demonstrated for NF-YA4/NF-YB3/NF-YC2, which regulates endoplasmic reticulum stress-induced genes (Liu and Howell, 2010). During senescence, NF-YA genes also show coordinated expression; however, they are overrepresented for upregulated genes (Breeze et al., 2011). The activity of the NF-Y complex could be regulated by the expression of either A, B, or C subunits; however, the coordinate regulation of NF-YA genes following both *B. cinerea* infection and during senescence suggests expression of A subunits may be an important control mechanism, as is the case in mammals (Manni et al., 2008).

Causal Structure Identification Network Modeling Highlights Potential Impact on Pathogen Growth

An advantage of extensive time series expression data is that it can be used in biological network inference: the prediction of the topology of a gene regulatory network. Understanding how genes interact and function together in networks to regulate plant responses is a crucial step toward being able to accurately predict the effect of genetic perturbations (i.e., phenotypic predictions from genotype). However, given the number of genes differentially expressed during *B. cinerea* infection, the number of time points and replicates in our data set are still insufficient to be able to generate a genome-wide network model; hence, the selection of genes to include in the model is necessary. As each cluster represents a group of coexpressed genes, we used the cluster mean as a representative of each group of genes and inferred network topology between the 44 clusters.

The expression of *B. cinerea* tubulin highlights two potential lag phases when pathogen growth appears to be arrested (Figure 2):

12 and 20 HAI. We compared this pathogen growth profile to the progression of transcriptional reprogramming in the host. Plotting the TOFDE obtained using the GP2S test indicates key times of transcriptional change; there is a small peak 11 HAI and a subsequent larger response beginning at 18 HAI (Figure 10). The two prospective lag phases in pathogen growth occur shortly after these peaks of transcriptional change, suggesting a possible causal relationship between transcriptional change in *Arabidopsis* and arrested growth of *B. cinerea*. To test this, we included the expression profile of *B. cinerea* tubulin (Figure 2), as an indicator of pathogen growth, in the network modeling. This *B. cinerea* growth profile was generated using the 12 observed levels of tubulin compared with *PUX1* (Figure 2) and interpolating over intermediate time points using Gaussian process regression (Rasmussen and Williams, 2006).

The discrete-time causal structure identification (CSI) algorithm of Klemm (Klemm, 2008; Penfold and Wild, 2011) was used to infer a regulatory network from the cluster means and *B. cinerea* growth. A section of the predicted network is shown in Figure 11, and several regulatory predictions can be made from this network. A single NAC TF, *ANAC055*, is present in cluster 23, and two clusters downstream of this (24 and 27) are enriched for a NAC binding motif in their gene promoter sequences. This suggests that ANAC055 regulates target genes in these clusters. Indeed, several genes differentially expressed in a knockout line of *ANAC055* compared with the wild type are present in cluster 27, including *ATG18a* (R. Hickman, C.L. Hill, S. Ott, and V. Buchanan-Wollaston, unpublished data). Furthermore, ANAC055 acts downstream of MYC2 in JA-mediated defense against *B. cinerea* (Bu et al., 2008), and clusters 24, 26, 27, and 28 are all overrepresented for genes differentially expressed in a *MYC2* knockout line ($P < 0.01$), suggesting this TF is a common upstream regulator. The activity of MYC2 is controlled by binding to JAZ proteins (Chini et al., 2009); consistent with this, *MYC2* is not differentially expressed during *B. cinerea* infection and hence is itself not included in any cluster.

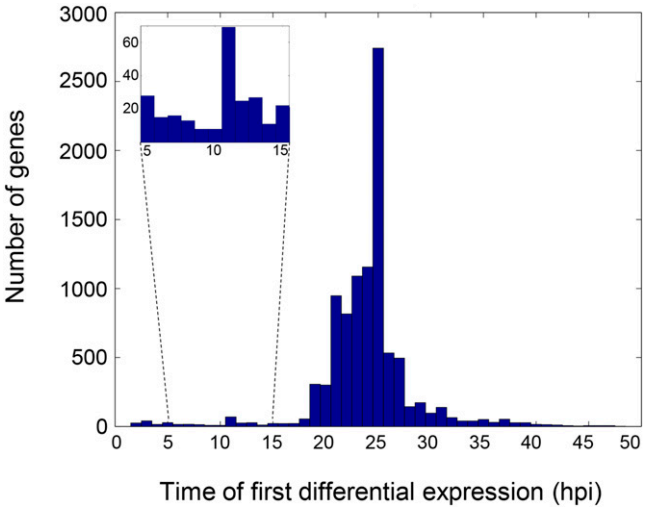

Figure 10. The Number of Genes First Differentially Expressed at Each Time Point.

TOFDE for all 9838 DEGs following infection with *B. cinerea* (HAI [hpi]) is shown. The inset shows early time points (5 to 15 HAI) in more detail. [See online article for color version of this figure.]

Two clusters (20 and 26) are enriched for genes containing MYB binding sites in their promoters (Figure 8) and are predicted to be downstream of clusters containing a MYB TF. Cluster 24 contains *MYB2* (a known stress-associated gene that plays a role in ABA signaling; Abe et al., 2003), and cluster 32 contains *MYB54*. MYB54 can induce genes of secondary cell wall biosynthesis (Zhong et al., 2008). Such genes are not overrepresented in cluster 20, but MYB54 may well have additional roles in the plant. Clusters 26 and 28 are enriched for W-box motifs and predicted to be downstream of cluster 24 containing *WRKY75*. *WRKY75* is known for its role in response to phosphate starvation but also influences basal and *R*-mediated defense against *P. syringae* (Encinas-Villarejo et al., 2009); hence, its predicted role in regulation of defense against *B. cinerea* is worth testing. The CSI network therefore has enabled predictions about the regulation of plant defense to be made. Although each node in the network represents a cluster of genes and hence the "causal" gene(s) in the node is not identified, specific hypotheses can be formed by integrating TF binding motif analysis.

In the CSI network model, growth of *B. cinerea* is upstream of at least nine clusters and is hence predicted to have a major effect on the transcriptome. Interestingly, pathogen growth is upstream of two clusters containing known clock genes, *LHY* and *GI* (clusters 6 and 34, respectively) potentially modeling the dampening of clock gene oscillations we observed in Figure 7. Only one cluster was found to be upstream of the *B. cinerea* growth curve, cluster 5. Cluster 5 contains two known TFs, *TGA3* and *ABF1*. Differential expression of *TGA3* starts around 18 HAI, shortly before the second pathogen lag phase, consistent with the hypothesis that downregulation of this TF may lead to the temporary arrest of pathogen growth. Therefore, we tested the effect of *TGA3* expression on susceptibility to *B. cinerea* using two independent knockout lines, *tga3-2* and *tga3-3*. Both mutant lines showed altered immunity, but surprisingly both knockout lines showed increased susceptibility to *B. cinerea* infection (Figure 12). However, the prediction of *TGA3* expression influencing *B. cinerea* growth from network modeling has led to identification of a new player in the defense response against this pathogen. More generally, the inclusion of phenotypic information into network inference may allow for important insights that could otherwise be missed.

Identification of TGA3-Regulated Genes during *B. cinerea* Infection

Having demonstrated that *TGA3* expression influences susceptibility to *B. cinerea*, we wanted to determine how TGA3 exerts its effect on defense by identifying the regulatory targets of this TF. The transcriptome of *tga3-2*–infected leaves was compared with *tga3-2* mock-inoculated controls and Columbia-0 (Col-0) infected leaves at three time points (16, 24, and 32 HAI). Genes differentially expressed between the wild-type and *tga3-2* infected leaves and between *tga3-2* mock-inoculated and infected leaves at one or more time points were compared with the 9838

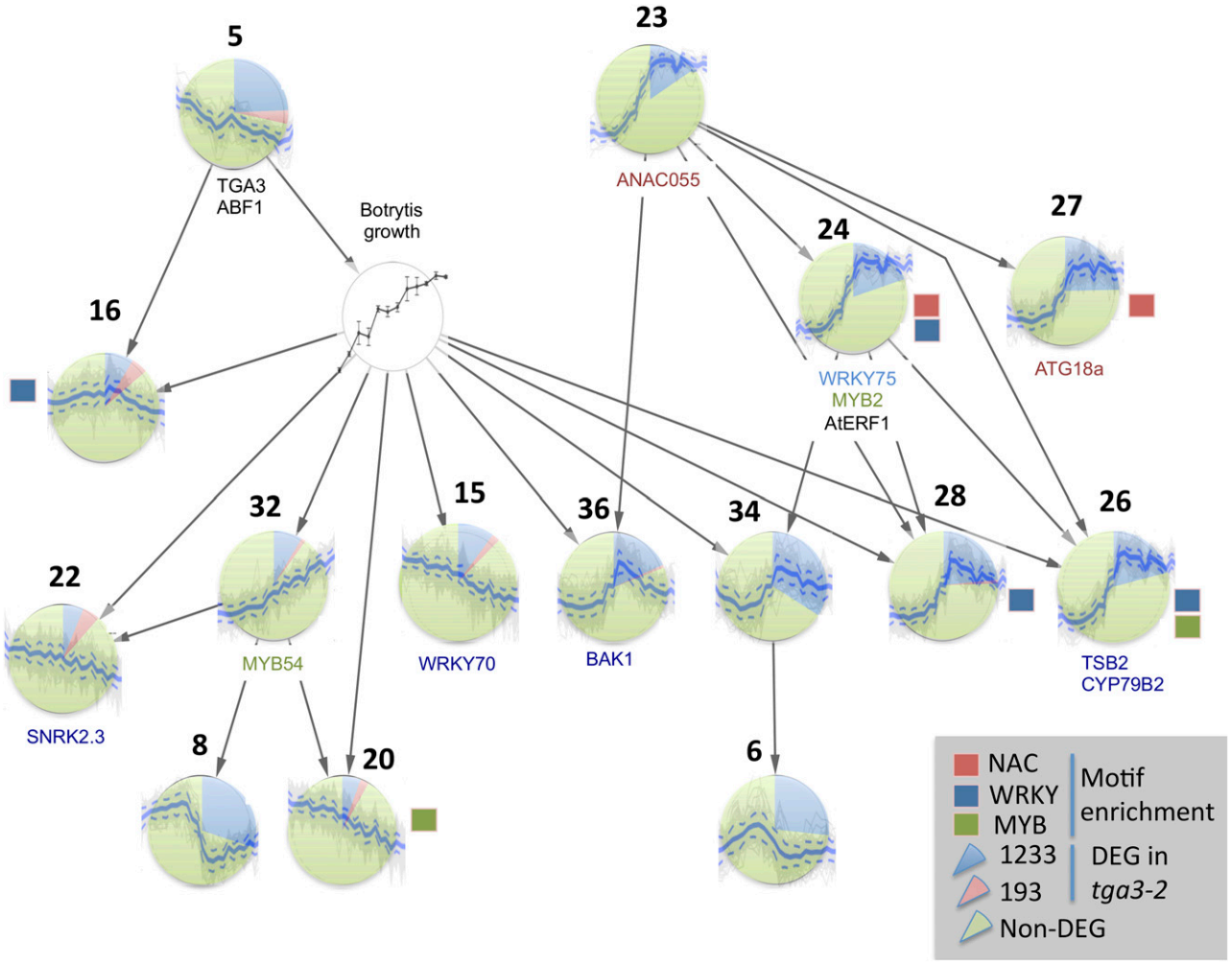

Figure 11. Inferred Network Model Using the Discrete-Time Causal Structure Identification Algorithm.

Numbered nodes represent a cluster from the SplineCluster clustering of genes differentially expressed during *B. cinerea* infection. The expression profile of *B. cinerea* tubulin was used as a proxy for pathogen growth. Selected TFs present in clusters are indicated under nodes. Colored boxes adjacent to nodes indicate motifs enriched in the promoter sequences of cluster genes, with TFs from the corresponding binding family highlighted in the same color. The color of nodes indicates the proportion of cluster genes that are differentially expressed in the *tga3-2* mutant compared with the wild type (either in the 193 or 1233 set of potential target genes).

DEGs from the time series (see Supplemental Figure 5 and Supplemental Data Set 11 online). A total of 2479 genes were differentially expressed between *tga3-2* and Col-0–infected leaves; 1426 of these are also differentially expressed in the time series infection data and hence are most likely to include target genes of TGA3 reproducibly regulated during *B. cinerea* infection. These 1426 genes can be partitioned into a group of 193 that are not differentially expressed between *tga3-2*–infected and mock-inoculated leaves (i.e., regulation during infection appears to be totally dependent on TGA3) and 1233 genes that are still differentially expressed between *tga3-2*–infected and mock-inoculated leaves. This latter group represents additional potential target genes of TGA3 with altered, but not abolished, expression in the knockout lines. As expected, *TGA3* fell into the group of 193. Looking at where *tga3-2* DEGs are in our network model (Figure 11), it is apparent that the 193 genes whose expression is totally dependent on TGA3 are more prevalent in groups of genes predicted to be downstream of cluster 5 (containing TGA3) or cluster 5 itself, than in cluster 23 (containing ANAC055) or groups predicted to be downstream of this cluster only.

The 1426 genes differentially expressed in *tga3-2* knockouts compared with the wild type during *B. cinerea* infection will contain both direct and indirect targets of TGA3. Screening upstream promoter sequences of these potential targets identified 395 genes that had one or more exact matches to the consensus binding sequence TGACGT in their promoters (see Supplemental Data Set 12 online). These represent the most likely direct targets of TGA3 and include *PR1*, a known target of TGA3 (Johnson et al., 2003). A few likely direct targets are worth

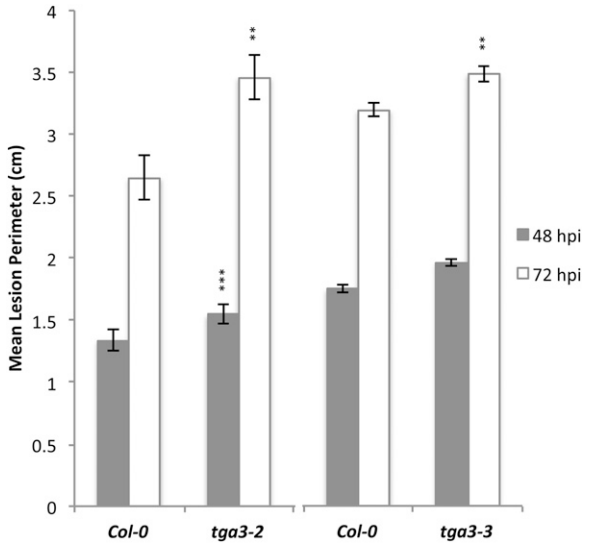

Figure 12. Susceptibility of *tga3* Mutants to *B. cinerea*.

Altered susceptibility of *tga3-2* and *tga3-3* T-DNA insertion lines compared with Col-0 control. Lesion perimeters are a mean of 20 leaves drop inoculated with 10 μL of 10^5 spores/mL of *B. cinerea*. Significantly different lesion perimeters in insertion lines compared with their respective Col-0 control were determined using a two-tailed Student's *t* test assuming equal variance. **P value < 0.001 and ***P value < 0.0001. Error bars show SE. hpi, hours post inoculation.

noting and are shown in Figure 11. Like *PR1*, expression of *WRKY70* is reduced in the *tga3-2* mutant compared with the wild type after *B. cinerea* infection. WRKY70 has a known role in defense and appears to integrate SA and JA responses (Li et al., 2006; Knoth et al., 2007). Two genes involved in the camalexin biosynthetic pathway (*TSB2* and *CYP79B2*) are both potential direct targets of TGA3 and are coexpressed during *B. cinerea* infection (Figure 11), suggesting a role for TGA3 in regulating this pathway. Two other potential direct targets of TGA3 (*BAK1* and *BRL3*) are highly upregulated during *B. cinerea* infection and may functionally interact. BAK1 is a Leu-rich repeat receptor kinase originally isolated through its role in brassinosteroid responses (dimerization with the Leu-rich repeat receptor kinase BRI1) (Li et al., 2002). BAK1 also dimerizes with FLS2, a pattern recognition receptor in plants, and absence of BAK1 increases susceptibility to biotrophic and hemibiotrophic pathogens (Roux et al., 2011). BRL3 is similar to BRI1 and has been shown to also bind brassinosteroids (Caño-Delgado et al., 2004). The positive regulator of ABA responses, *SNRK2.3*, is upregulated in the *tga3-2* mutants compared with the wild type and contains a motif matching the TGA consensus within its upstream sequence. As with other ABA signaling components, *SNRK2.3* is downregulated during *B. cinerea* infection, and TGA3-mediated expression appears to be one mechanism for this. Interestingly, this target gene analysis suggests two potential regulatory mechanisms of TGA3 itself. At a protein level, TGA3 interacts with NPR3; *NPR3* is downregulated in *tga3-2* mutants compared with the wild type and its promoter contains a TGA binding site. Similarly, the promoter of *TGA3* contains a TGA binding site, suggesting autoregulation or regulation by other TGA factors. Despite including clear defense-related genes, the TGA3 target genes are enriched for annotation with the GO terms "response to abiotic stimulus," "response to oxidative stress," and "response to water deprivation," suggesting TGA3 may play a wider role in plant responses to stress.

DISCUSSION

Timing of Differential Gene Expression

We have presented a high-resolution time series of gene expression during infection of *Arabidopsis* leaves by the fungal pathogen *B. cinerea*. Analysis of this transcriptome time series has shown that approximately one-third of the *Arabidopsis* genome changes in expression during the first 48 h after infection. Within this, we have identified groups of genes activated or repressed at different times. The identification of genes differentially expressed due to *B. cinerea* infection was not trivial. When used to determine differential expression between two conditions (mock inoculated and infected) over time, the *timecourse* algorithm produced a large number of clear false positives. On the other hand, a straightforward F test appeared to have a high false negative rate, identifying far fewer genes as differentially expressed compared with *timecourse* and GP2S. The GP2S method, fitting Gaussian processes to the two conditions separately and jointly and assessing which fits the data better, identified many DEGs with an acceptable false positive rate. A small group of genes with true differential expression were only identified using the F test. This group contained several genes expressed in a diurnal manner; it appears that the GP2S algorithm with the standard choice of covariance function and inference is reluctant to fit expression profiles with multiple changes over the 48-h period. The method could probably be adapted to better accommodate these specific genes by means of a change in window size (length-scale) or the inference method used.

One striking finding from our analysis of DEGs is that the majority of changes in gene expression have occurred by 24 HAI when the pathogen has penetrated the leaf epidermis but only very small, localized lesions are present. Transcriptome profiling was performed on whole leaves inoculated with five to seven droplets of *B. cinerea* spores (for example, Figure 2); hence, at 24 HAI, very little leaf tissue is adjacent to the invading fungus. This would suggest that either the changes in gene expression are so extreme in the cells adjacent to the pathogen or, more likely, that signals from the pathogen and/or plant spread out from the site of penetration and initial lesion formation causing gene expression changes over a larger leaf area. Consistent with this, published analyses of the *Arabidopsis* transcriptome after *B. cinerea* infection have shown that leaves inoculated with a single droplet of spores exhibit significant transcriptome change (Rowe et al., 2010) and large numbers of genes were differentially expressed in tissue 6 to 12 mm from a *B. cinerea* lesion compared with mock-inoculated controls (Mulema and Denby, 2012). This latter study also highlighted the spatial aspect of the response to *B. cinerea* infection, with significant numbers of genes being differentially expressed in tissue either

1 to 6 or 6 to 12 mm from the lesion. Although we sampled whole leaves, we may have captured some of this spatial response over time due to the radial nature of lesion development; over time, increasing amounts of tissue are recruited to these spatial regions.

Despite sampling every 2 HAI, the majority of gene expression changes occur in a relatively small time window (~18 to 30 HAI) focused around the lag phase in pathogen growth, when the infection changes from penetration of the host and primary lesion formation to lesion expansion within the host. This correlation could be viewed as a response (too late) of the plant to the change in attack strategy of the pathogen or the response of the plant may cause the temporary halt in pathogen growth. A finer time resolution of expression profiling over this period may resolve these two alternatives, along with careful monitoring of pathogen growth in mutants of key components regulating these changes in expression. A finer time resolution across this period would also improve the ability of modeling algorithms to predict gene–gene interactions.

We observed dampening of expression of core clock components from ~24 HAI. Given the emerging role of the clock in defense, this may reflect an attempt by the pathogen to dampen rhythmic defense gene expression. A more prosaic explanation is that the clock is more sensitive to changes in the rate of protein synthesis due to the relatively rapid changes in protein levels needed to drive clock oscillations. Genes involved in translation are overrepresented in downregulated genes at multiple time points from 12 HAI onwards. If this downregulation leads to reduced levels of translational machinery, and a reduced rate of protein synthesis, this may explain the dampening of clock gene expression. The plant may also redirect resources from the clock toward defense.

Sequential Involvement of Plant Hormones in Defense against *B. cinerea*

Although much of the *Arabidopsis* genome is not annotated with GO terms, the use of overrepresentation to dissect a biological process is still useful. The association between GO terms and specific clusters of genes has enabled us to separate different components of the defense response against *B. cinerea* in time. We identified early responses, some of which have not been implicated in defense against *B. cinerea* before, and highlighted novel groups of genes that may play a role in reducing susceptibility to this pathogen. Coexpression of genes with a related function over a highly resolved time series strengthens the likelihood of such a function being important.

Plant hormones are known to influence each other's effects, both positively and negatively. The relative timing of plant hormone action during the defense response against *B. cinerea* can highlight points of interaction and help resolve sometimes contradictory results about the influence of individual hormones on susceptibility to this pathogen. Genes involved in the synthesis of ET were highlighted by our GO term analysis and began to change at 14 HAI, with "response to ET" genes changing in expression remarkably quickly, a mere 2 h later (Figure 4). At the same time (16 HAI) JA-responsive genes were overrepresented, suggesting prior JA synthesis. Looking at the expression data, the vast majority of genes encoding enzymes of JA biosynthesis were upregulated between 12 and 14 HAI, suggesting synthesis of JA occurs when expected, and consistent with upregulation of JA biosynthetic genes at 14 HAI by Birkenbihl et al. (2012). However, a single member of the allene oxide cyclase family, *AOC4*, and one of the four lipoxygenase genes, *LOX2*, are downregulated in response to infection from 20 HAI. *LOX1* is upregulated but again only at this late stage. Why these three genes are regulated in such a different manner to the rest of the pathway is not clear but presumably reflects distinct roles in the synthesis of JA in response to different stimuli and/or in different tissues. The ability to see these differences in expression over time is providing a more nuanced picture of hormone involvement, and integrating such data from multiple treatments could help elucidate precise roles of specific gene family members. The early activation of JA and ET biosynthetic genes suggests that their expression is mediated by MAMP/DAMP recognition, and JA biosynthetic genes are rapidly induced after treatment of seedlings with OGs (Denoux et al., 2008), a DAMP signal generated during *B. cinerea* infection. Notably, it is *LOX3* and *LOX4* (the two rapidly upregulated LOX genes in our time series) that are induced in response to OGs, strengthening our hypothesis that these two are responsible for this early JA response.

Our analysis of overrepresented GO terms highlighted auxin biosynthesis occurring after ET (and JA) synthesis with ET potentially acting as a trigger for this process. At a similar time during infection, genes involved in the suppression of ABA accumulation and signaling were upregulated. The role of ABA in biotic stress is complex with both positive and negative effects on plant defense reported (Asselbergh et al., 2008; Ton et al., 2009). Ton et al. (2009) attempted to characterize these interactions as dependent on the stage of infection and pathogen kingdom, with ABA having a positive role in early postinvasive defense against fungi and a negative role against bacteria. However, ABA appears to have a negative effect on defense against *B. cinerea* with ABA-deficient mutants in both tomato (*Solanum lycopersicum*; Audenaert et al., 2002) and *Arabidopsis* (Adie et al., 2007) being less susceptible to this pathogen. ABA signaling mutations also decrease susceptibility. Some isolates of *B. cinerea* are able to make ABA (Siewers et al., 2006) and may use this hormone as an infection strategy to manipulate the host defense response. Active repression of downstream signaling by the host may therefore be required for successful defense with upregulation of both ABA catabolic genes and negative regulators of ABA signaling reflecting the need of the plant to dampen ABA responses rather than simply reduce ABA accumulation.

ABA can function as a repressor of SA-, ET-, and JA/ET-dependent signaling but appears to act positively on some JA responses (possibly those activated via MYC2) (Asselbergh et al., 2008; Ton et al., 2009). As both ERF1 and ORA59, the key regulators of JA/ET signaling, positively influence defense against *B. cinerea* (Berrocal-Lobo et al., 2002), repression of ABA signaling should again increase defense against this pathogen.

Lastly, around 22 HAI SA biosynthetic genes are downregulated. The SA and JA pathways are known to be mutually antagonistic, and the relative timing of biosynthetic gene expression suggests that during the defense response against

B. cinerea, earlier JA synthesis leads to downregulation of the SA pathway. The role of SA signaling in defense against *B. cinerea* is not completely clear. JA and ET responses are often found to be more important in defense against necrotrophic pathogens, but a study by Ferrari et al. (2003) demonstrated that exogenous application of SA decreased susceptibility while plants expressing the NahG transgene (which reduces SA levels) or treated with a phenylalanine ammonium lyase (PAL) inhibitor had increased susceptibility. SA can be synthesized via PAL or isochorismate synthase (ICS), and mutants defective in ICS1 had wild-type levels of susceptibility to *B. cinerea*. These data would point to SA synthesized via PAL having a protective role against *B. cinerea*. Priming with SA, or its functional homolog benzo-(1,2,3)-thiadiazole-7-carbothioic acid *S*-methyl ester, reduces susceptibility to *B. cinerea* if treatment occurs 1 but not 2 d prior to infection (Zimmerli et al., 2001; Govrin and Levine, 2002). This could indicate that timing of SA signaling is important; our expression data suggest that basal levels of PAL are sufficient for early synthesis of SA and that synthesis of this hormone is downregulated as infection progresses.

It is also possible that host processes are activated or repressed by the pathogen in order to cause disease. Overrepresentation of the GO term "protein phosphorylation" at 20 HAI highlighted a group of five receptor-like protein kinases downregulated during infection. This group includes FLS2, which mediates MAMP-triggered basal immunity, leading to the hypothesis that downregulation of these receptor-like protein kinases is driven by the pathogen to dampen activation of the immune response.

A Role for TGA3 in Defense against Necrotrophic Pathogens

TGA TFs are known for their role in SA-dependent signaling. SA induces redox-dependent phosphorylation of NPR1, leading to translocation of NPR1 to the nucleus where it binds to TGA factors enhancing their ability to bind SA-responsive promoters (Loake and Grant, 2007). Within the TGA family, TGA3 binds most strongly to NPR1, and *tga3* mutants have reduced expression of *PR1* and increased susceptibility to the bacterial pathogen *P. syringae* (Kesarwani et al., 2007). Often mutations that increase susceptibility to biotrophic or hemibiotrophic pathogens reduce susceptibility to necrotrophic pathogens and vice versa, thought to be due to the SA-JA antagonism. However, here, we have shown that reduced expression of *TGA3* leads to increased susceptibility to both types of plant pathogen. The triple *tga2 tga5 tga6* mutant is defective in JA responses and also exhibits increased susceptibility to *B. cinerea* but unlike *tga3* does not show altered basal resistance to *P. syringae* (Zhang et al., 2003; Zander et al., 2010). It seems likely that the SA signaling role of TGA3 is less important following *B. cinerea* infection and that TGA3 is playing additional regulatory roles. Indeed, GO terms relating to SA, JA, ABA, and ET are all overrepresented in the 1426 *B. cinerea*–responsive genes differentially expressed in *tga3-2* mutants compared with the wild type, suggesting that TGA3 acts as a key node in hormone regulation of the defense response. Potential direct targets of TGA3 include the ABA signaling genes *SNRK2.3* and *MYB2*, as well as *WRKY70*, which mediates SA–JA interactions (Figure 11), lending weight to this hypothesis. Our analysis of TGA3 target genes also indicates that TGA3 acts as both an activator and repressor of gene expression (Figure 11).

Intriguingly, T-DNA insertion lines with reduced expression of *TGA3* show increased susceptibility to this pathogen, although *TGA3* is downregulated during *B. cinerea* infection in wild-type plants. There are several explanations: The expression profile could reflect pathogen suppression of this defense gene, or the precise level of TGA3 protein and/or spatial and temporal expression of this gene could be crucial to its function in defense. Although we have a high-resolution time series data set, the profiles are obtained from whole leaves, hence losing all cell type differences in gene expression. Obtaining expression data from specific cell types over time could identify a number of expression differences in key genes between cell types and hence help to resolve TGA3 function, as well as highlight other important defense mechanisms.

Network Modeling Enables Prediction of Regulatory Interactions

While GO term analysis of coexpressed clusters can elucidate the chronology of biological processes, modeling of such clusters combined with motif analysis can generate regulatory predictions for such processes. For example, cluster 27 is overrepresented for genes involved in autophagy and overrepresented for genes containing a NAC motif in their promoters. Upstream of cluster 27 in our CSI network model is cluster 5 containing a single NAC TF, *ANAC055*. Expression data from a knockout of *ANAC055* indicated that the autophagy gene ATG18a is downstream of *ANAC055*. The known role of ANAC055 in JA responses mediated by MYC2 generates the hypothesis that JA signaling mediates autophagy during *B. cinerea* infection. The edges in the CSI network (Figure 11) are predicted gene–gene (or cluster–cluster) interactions. They are not necessarily direct interactions, so although the *ATG18a-ANAC055* interaction stood out from motif analysis, many more regulatory relationships could be captured in this model.

We know that plant defense is characterized by major transcriptional reprogramming and the time series expression data in this article can be used with a variety of algorithms to generate models of the transcriptional gene regulatory networks underlying the defense response against *B. cinerea*. The alternative type of expression data, static data, can also be informative if perturbations to the system are included. Such data (single time point analysis in a large number of mutant backgrounds) has been used successfully to generate network models of the defense response to *P. syringae* infection predicting known regulatory relationships (Sato et al., 2010). Although static data from specific perturbations can be used to filter dynamic network models, as we have done in this article, the ability to combine dynamic and static data is likely to dramatically enhance the predictive capacity of gene regulatory models.

Although we identified clusters of genes overrepresented for specific known TF binding sites and generated several specific hypotheses about TF action, the ability of this approach to lead to network reconstruction is limited by our lack of knowledge of the specificity conferred by particular motifs. We have little

understanding of how DNA sequence surrounding a core motif determines which clade or individual TF within a family can bind, and for many families of TFs, we do not even know a core motif. The bottleneck is the number of experimentally confirmed direct TF–DNA interactions. This is highlighted by a recent literature survey performed using The Arabidopsis Information Resource, PubMed, iHOP, and ONDEX. We surveyed 628 TF genes, but only 72 of these had any experimentally confirmed (ChIP, yeast one-hybrid, or in vitro binding assays) direct TF–promoter interactions. The onset of matrix-style yeast one-hybrid analysis and growing amounts of ChIP-seq data will dramatically increase the number of direct TF–DNA interactions in the literature and, hence, our ability to discern how promoter sequences encode specificity and our capacity to predict additional interactions.

We are well aware that transcriptional regulation is not the only mechanism of gene regulation in plants, and examples of post-transcriptional or posttranslational regulation abound; WRKY33 is one well-studied example where initial activation of this TF is mediated by phosphorylation. The next challenge is to link nontranscriptional regulation to transcriptional network models, with potential inputs including MAP kinase signaling, calcium and calmodulin signaling, activation of membrane-bound TFs, and phosphor-relay downstream of His kinases. Specific MAP kinases and a putative His kinase are already known to affect susceptibility to *B. cinerea* (Galletti et al., 2011; Pham et al., 2012) with modulation of downstream gene expression a likely cause of these phenotypes.

We have generated high-resolution times series expression data and used these in a variety of computational tools to obtain a detailed picture of the order of biological processes and signals during defense against *B. cinerea*, identify novel regulators of this defense response, and make regulatory predictions for experimental testing. With the advent of sequencing-based expression profiling and availability of *B. cinerea* genome sequence (Amselem et al., 2011), it becomes feasible to generate time series gene expression data simultaneously for host and pathogen. Integrating transcriptional network models from host and pathogen could highlight specific points of interaction between the two organisms, as well as drive identification of novel pathogen targets for chemical control.

METHODS

Plant and Fungal Growth and Plant Infection

Arabidopsis thaliana plants (Col-0, *tga3-2* [SALK_086928c], and *tga3-3* [SALK_088114]), obtained from the Nottingham Arabidopsis Stock Centre, were grown under a 16:8-h light:dark cycle at 23°C, 60% humidity, and light intensity of 100 μmol photons·m^{-2}·s^{-1}. *Arabidopsis* seed was stratified for 3 d in 0.1% agarose at 4°C before sowing onto *Arabidopsis* soil mix (Scotts Levingtons F2s compost:sand:fine grade vermiculite in a ratio of 6:1:1).

Botrytis cinerea strain pepper (Denby et al., 2004) was subcultured on sterile tinned apricot halves in Petri dishes 2 weeks prior to use of the spores. Subcultures were incubated in the dark at 25°C. Spore inoculums were prepared by harvesting spores in water, filtration through glass wool to remove hyphae, and suspension in half-strength sterile grape juice to a concentration of 10^5 spores/mL.

For time series expression analysis, leaf 7 was tagged on 192, 25-d-old plants. Three days later, leaf 7 from each of these plants was detached and placed on a bed of 0.8% agar in four propagator trays. Half of the leaves were inoculated with five to seven (depending on the size of the leaf) 10-μL droplets of *B. cinerea* inoculum so that droplets were evenly spaced over the leaf. The remaining 96 leaves were mock inoculated with five to seven 10-μL droplets of sterile half-strength grape juice. Each tray contained 24 infected and 24 uninfected leaves randomly arranged. Trays were covered with lids and kept under the same conditions as for plant growth, except the relative humidity was raised to 90%. Leaves were inoculated 6 h after dawn. Single infected and control leaves were sampled in a randomized manner from each of the four trays every 2 h over 48 h. This gave four biological repeats (i.e., four individual leaves) for both infected and control treatments at each of the 24 time points. Whole leaf samples were snap frozen in liquid nitrogen at the time of harvesting and stored at −80°C. The same protocol was followed for expression analysis in *tga3-2* plants except that leaves of *tga3-2*–infected, *tga3-2* mock-infected, and Col-0–infected plants were harvested. This was done at 16, 24, and 32 HAI.

For assaying susceptibility of plant lines, Col-0, *tga3-1*, and *tga3-2* were grown and infected as above, except that a single 10-μL droplet of *B. cinerea* inoculum or sterile half-strength grape juice (mock control) was placed in the center of each leaf. Lesion perimeters were determined from photographs taken 48 and 72 HAI using the image analysis software ImageJ 1.40g (http://rsb.info.nih.gov/ij/). Mean lesion perimeters of 20 leaves from 20 plants of T-DNA lines and Col-0 were compared using a Student's two-tailed *t* test assuming equal variance.

RNA Extraction, Amplification, and Microarray Experiments

Total RNA was extracted, labeled, and hybridized to CATMA v3 arrays (Sclep et al., 2007) as previously described (Breeze et al., 2011), other than two separate rounds of cDNA synthesis, which were performed in parallel for each infected sample, pooled, and used in a single 14-h in vitro transcription incubation. The experimental design for the time series is shown in Supplemental Figure 1 online.

Following the 16-h hybridization, arrays were washed once in wash solution 1 (25 mL 20× SSC, 1.8 mL 14% [w/v] SDS, and 223 mL water) preheated to 42°C for 5 min on an orbital shaker, and wash solution 2 (1.25 mL 20× SSC, 1.8 mL 14% [w/v] SDS, and 247 mL water) for 10 min on an orbital shaker, then four times in wash solution 3 (5 mL 20× SSC and 995 mL water) for 1 min on an orbital shaker. After washing, arrays were briefly immersed in isopropanol then spun dry. Arrays were scanned on a 428 Affymetrix scanner at wavelengths of 532 nm for Cy3 and 635 nm for Cy5. Cy3 and Cy5 scans for each slide were combined and processed in ImaGene version 8.0 (BioDiscovery) to extract raw intensity and background corrected data values for each spot on the array. The full data set is available in GEO under accession number GSE29642 (part of SuperSeries GSE39598).

For the *tga3-2* expression analysis, amplified RNA samples from four biological replicates were pooled. *tga3-2* infected samples were directly compared with *tga3-2* mock-infected and Col-0–infected samples within, but not between, each time point. Each comparison had four technical replicates, including two dye swaps with 24 arrays performed in total using CATMA v4 arrays (Sclep et al., 2007). The data set is available in GEO under accession number GSE39597 (part of SuperSeries GSE39598).

Analysis of Microarray Data

A local adaptation of the MAANOVA package (Wu et al., 2003) was used to analyze the extracted microarray data as described by Breeze et al. (2011), using a mixed-model analysis. The MAANOVA fitted model considered dye and array slide as random variables, and time point, treatment and biological replicate as fixed variables. The model allowed assessment of the main effect of treatment, the main effect of time point,

the interaction between these factors, and the nested effect of biological replicate. Predicted means were calculated for each gene for each of the 192 combinations of treatment, time point and biological replicate, and for each of the 48 combinations of treatment and time point (essentially averaging across biological replicates). The expression data were normalized on a per gene basis either across the whole experiment or for the *B. cinerea*–infected time points only depending on the analysis being performed.

Approximate F tests, constructed from the fitted models for each gene, were used to assess each gene for significant changes in expression associated with treatment and the interaction between treatment and time point. The Benjamini and Hochberg false discovery rate (FDR) multiple testing correction (Benjamini and Hochberg, 1995) was applied. This identified 6512 DEG probes using a cutoff of adjusted $P < 0.05$. A GP2S (Stegle et al., 2010) and a Hotelling statistic (T^2) proposed by Tai and Speed (2006) were used to rank genes in order of likelihood of differential expression. Manual inspection of the expression profiles of every 100th gene in the GP2S ranking, and subsequently of all genes ranked 10,400 to 11000, was used to decide on a cutoff of 10,600 DEGs. Below this, the proportion of clearly non-DEGs increased dramatically. The top 10,600 genes ranked by T^2 were also selected and used in a comparison with GP2S and the F test (see Supplemental Figure 2 online). The majority of genes identified by the F test were also ranked above 10,600 in both GP2S and T^2. However, significant numbers of genes were identified only by GP2S and/or T^2. Inspection of the expression profiles for these groups of genes revealed that the T^2 statistic identified a large number of genes whose expression was clearly not differentially expressed yet were highly ranked. By contrast, the number of clear false positives in the GP2S only category was very low (see Supplemental Figure 2 online). The 236 genes identified by the F test and not GP2S contained many genes clearly differentially expressed when manually inspected. On this basis, it was decided to combine the top 10,600 gene probes ranked by GP2S with the 236 additional gene probes identified by the F test. Expression profiles of three sets of 350 gene probes, those ranked 8800 to 9149, 9450 to 9799, and 10,200 to 10,549 in the GP2S, were manually inspected. The percentage of clear false positives was 6, 10, and 18%, respectively (i.e., the higher the ranking of the genes, the lower the percentage of clear false positives). As we wanted a comprehensive view of gene expression during infection and, from the rates mentioned, the number of false positives above the conventional 5% threshold is likely to only be a couple of hundred, further manual inspection of the 10,836 gene profiles was not performed. Following annotation using TAIR9, 371 profiles were removed as they did not hybridize to open reading frames. A total of 627 duplicate probes (i.e., two or more probes mapping to the same gene) were removed with the best probe as determined by BLAST score kept for each duplicate.

For the *tga3-2* expression analysis, the arrays from each time point comparison were analyzed as separate experiments using the R Bioconductor package limmaGUI (Wettenhall and Smyth, 2004). Raw data were first adjusted using a PrintTip lowess transformation before scaling to normalize between arrays. A least squares method was used to fit the data to a linear model. In each time series, genes were selected as differentially expressed if the adjusted P value (Benjamini and Hochberg FDR; Benjamini and Hochberg, 1995) was <0.05 for a moderated *t* test of the $\log_2$ relative expression.

Mapping of CATMA v4 probes to *Arabidopsis* gene models was performed as described for CATMA v3 (Breeze et al., 2011) with some manual curation to identify the best mapping where several possible mappings were suggested by the analysis.

RT-PCR

cDNA was made from amplified RNA for three biological replicates of alternate time points from the time series experiment (i.e., every 4 h over 48 h). This cDNA was used as a template in relative quantitative RT-PCR to compare *B. cinerea* tubulin (*Bc Tub*; Broad MIT ID: BC1G_00122) mRNA levels using primers 5′-TTCCATGAAGGAGGTTGAGG-3′ and 5′-TACCAACGAAGGTGGAGGAC-3′, to *PUX1* (At3g27310) expression using primers 5′-TTTTTACCGCCTTTTGGCTA-3′ and 5′-ATGTTGCCTCCAATGTGTGA-3′. *PUX1* was shown in the microarray analysis not to change significantly over 48 h between infected and mock-infected leaves. The expression of *LOX2* (At3g45140) and *ANAC002/ATAF1* (At1g01720) relative to *actin* was also determined across the original time series experiment (8, 12, 16, 20, 24, 28, 32, and 36 HAI) in both mock and infected samples using quantitative RT-PCR with primers 5′-TCCCCAAGAACCTTTTCCAC-3′ and 5′-ACTCGTCGTCTCGTAACCAT-3′ (*LOX2*), and 5′-CGAAATCATGGAGGAGAAGC-3′ and 5′-TGTCGAAATACGCGAACTCA-3′ (*ANAC002/ATAF1*).

The transgenic lines *tga3-2* and *tga3-3* were shown to have reduced expression of the *TGA3* gene by RT-PCR on leaves from 4-week old plants using primers 5′-TGAAGCAGAACCGTCGAGTA-3′ and 5′-TGCGTAGTGGTTCAAGCAAC-3′ for the *TGA3* gene and primers 5′-GCCATCCAAGCTGTTCTCTC-3′ and 5′-CAGTAAGGTCACGTCCAGCA-3′ for actin (At3g18780). Both lines exhibited reduced *TGA3* expression (see Supplemental Figure 6 online), although *tga3-3* showed highly variable expression.

In all cases, cDNA was made using Superscript Reverse Transcriptase II (Invitrogen) with random hexamers, following the manufacturer's instructions, and PCR performed in triplicate using SYBR Green PCR Master Mix (Applied Biosystems) in a Roche-LightCycler 480 Real-Time PCR system following manufacturer's suggested running conditions.

Clustering of Gene Expression Profiles

Clustering of DEGs was performed using SplineCluster (Heard et al., 2005) using the expression profiles generated in MAANOVA combining the four biological replicates. DEGs were clustered using a prior precision value of 0.001. An additional reallocation function (Heard, 2011) that reassessed clusters at each agglomerative step to reallocate cluster outliers into more appropriate clusters was also implemented.

GO Analysis

GO annotation analysis was performed using the BiNGO 2.3 plugin tool in Cytoscape version 2.6 with the GO_Biological_Process category, as described by Maere et al. (2005). Overrepresented GO_Biological_Process categories were identified using a hypergeometric test with a significance threshold of 0.05 after Benjamini and Hochberg FDR correction (Benjamini and Hochberg, 1995) with the whole annotated genome as the reference set.

Expression Profile Analysis

Genes that were differentially expressed during *B. cinerea* infection were identified using the GP2S method (Stegle et al., 2010). The time at which each of these genes first became differentially expressed (TOFDE) was subsequently determined using the GP2S time-local method (Stegle et al., 2010). To define the time of expression change for a cluster, a gradient analysis was applied to each DEG as by Breeze et al. (2011). This gives a value of -1 (significantly downregulated), 0 (not changing), or 1 (significantly upregulated). The time of expression change for a cluster was defined as the point at which the absolute average value for the genes in the cluster was ≥ 0.5. Genes that exhibited rhythmic expression were identified using JTK_CYCLE and default parameters (Hughes et al., 2010). Up- or downregulation for genes differentially expressed in response to *B. cinerea* infection was determined by calculating the difference between infected and mock-inoculated expression values. With the exception of 153 genes, this corresponded to clusters 23 to 44 being classed as upregulated and clusters 1 to 22 being classed as downregulated. As 153 genes is a small proportion of the DEGs (9838), the cluster classifications were used for this analysis.

Promoter Motif and TF Family Analysis

Analysis of overrepresented TF binding motifs in promoter sequences was performed exactly as described by Breeze et al. (2011). The 500 bp of sequence upstream of the transcriptional start site was tested. For promoter analysis of potential TGA3 target genes, a TGA positional weight matrix (M01815) was obtained from TRANSFAC (Matys et al., 2006). Upstream promoter sequences of length 2 kb (or up to the nearest neighboring gene if closer than 2 kb) for the 1426 genes differentially expressed in *tga3-2* compared with the wild type following infection with *B. cinerea* were extracted from a local Ensembl database (corresponding to the TAIR9 annotation). Sequences were searched for motif matches using the method outlined by Breeze et al. (2011). For each promoter sequence, the best 10 matches to the motif were obtained, ranked by score (Kel et al., 2003), and exact matches to the 6-mer core binding sequence (TGACGT) recorded.

Gene expression was analyzed for 1850 TFs, grouped into 50 families defined in the *Arabidopsis thaliana* Transcription Factor Database (Palaniswamy et al., 2006), using the GP2S time-local model. A threshold of $P \geq 0.5$ was used to determine differential expression at a given time, and mode of differential expression (up- or downregulated) is inferred from the transcript data. Families overrepresented for DEGs at each time bin (time is binned into 2 h, starting at 2 h post infection), using all genes mapped to a probe on the arrays as a reference, were identified using the hypergeometric distribution with FDR correction (Benjamini and Hochberg, 1995). A heat map of adjusted P values, using five levels of significance (0.01, 0.05, 0.1, 0.25, and 0.5), was then generated, showing families only if they have at least one adjusted P value < 0.1.

Network Modeling Using Causal Structure Identification

The mean of each cluster was taken as being representative of that particular cluster and a network inferred using CSI (Klemm, 2008; Penfold and Wild, 2011). An additional node in the network representing *B. cinerea* tubulin expression during infection was included. Since tubulin expression was measured over a subset of time points (Figure 2), intermediate measurements were interpolated as the mean of an independent Gaussian process regression with squared exponential covariance function and additive white noise. Hyperparameters were set to maximize the marginal likelihood with initial values randomly selected from a zero-mean, unit-variance normal distribution.

Within the CSI inference procedure, the maximum number of parents that could bind simultaneously was set to 2. The covariance function was again chosen to be the squared exponential with white noise and hyperparameters chosen to maximize the marginal likelihood using an expectation maximization algorithm. Several runs of the expectation maximization algorithm were performed to ensure convergence. Finally, the network structure was summarized by calculating the marginal probabilities for each prospective parent to yield a fully connected graph. The network was subsequently made sparser by setting all links with a marginal probability below 0.15 to 0.

TGA3 T-DNA Knockout Genotyping

TGA3 T-DNA insertion lines were screened for presence of the T-DNA in the *TGA3* gene using the following gene-specific primers: *tga3-2*, 5′-CCACTCTTGTCCCACAAAATG-3′ and 5′-TCCATATCTCTAAAATTGCATTGC-3′; *tga3-3*, 5′-CTGCATAGCACTGAGACCCTC-3′ and 5′-GAAAACCCAGCTCTCCAAAAC-3′; with the appropriate T-DNA–specific primer (SALK, LBa1 5′-GCGTGGACCGCTTGCTGCAACT-3′, SAIL, LB1 5′-GCCTTTTCAGAAATGGATAAATAGCCTTGCTTCC-3′, and GABI-Kat 08409 5′-ATATTGACCATCATACTCATTGC-3′). The control lines for analysis of *B. cinerea* susceptibility were two Col-0 wild-type lines isolated from two segregating T-DNA SALK lines (but not the TGA3 lines) using PCR-based screening methods.

MYC2 Transcriptome Comparison

A list of 778 genes differentially expressed in a *MYC2* knockout compared with the wild type was obtained from Dombrecht et al. (2007) Overrepresentation of these genes in the gene lists from individual clusters was assessed using the cumulative hypergeometric distribution relative to the background of the 23,802 unique genes represented on CATMA v3 arrays. This analysis was performed in MATLAB R2010a using the script hygepdf.m.

Accession Numbers

GEO SuperSeries GSE39598 contains the raw data files and processed normalized expression data from the *B. cinerea* time series experiment (accession number GSE29642) and the *tga3-2* expression profiling (accession number GSE39597). The Arabidopsis Genome Initiative numbers corresponding to *Arabidopsis* gene names mentioned in the text are given in Supplemental Table 2 online: Germplasm *tga3-2* (SALK_086928c) and *tga3-3* (SALK_088114).

Supplemental Data

The following materials are available in the online version of this article.

Supplemental Figure 1. Experimental Design for the Microarray Hybridizations.

Supplemental Figure 2. Identification of Differentially Expressed Genes.

Supplemental Figure 3. Comparison of Gene Expression in This Study and Literature after *B. cinerea* Infection.

Supplemental Figure 4. Time Series Expression Profiles of the 9838 Differentially Expressed Genes during Infection Clustered Using SplineCluster.

Supplemental Figure 5. Identification of Genes Potentially Regulated by *TGA3* during *B. cinerea* Infection.

Supplemental Figure 6. Expression of *TGA3* in the Wild Type, *tga3-2*, and *tga3-3*.

Supplemental Table 1. Comparison of Gene Expression Profiles Following *B. cinerea* Infection from the Literature and This study.

Supplemental Table 2. AGI Identifiers for All Genes Mentioned by Name in the Text.

Supplemental Data Set 1. Membership of Gene Clusters.

Supplemental Data Set 2. GO Biological Process Terms Significantly Overrepresented in the 44 Gene Clusters Generated by SplineCluster from Infected Leaf Expression Profiles.

Supplemental Data Set 3. GO Biological Process Terms Significantly Overrepresented in Gene Clusters Generated from Time of First Differential Expression Following *B. cinerea* Infection of Leaves.

Supplemental Data Set 4. Lists of Genes Obtained by Comparing Genes Differentially Expressed during Senescence and *B. cinerea* Infection.

Supplemental Data Set 5. GO Terms Significantly Overrepresented in the Sets of Genes Obtained by Comparing Genes Differentially Expressed during Senescence and *B. cinerea* Infection.

Supplemental Data Set 6. Genes Rhythmically Expressed in *Arabidopsis* Mock-Inoculated Leaves with a Period between 20 and 28 h.

Supplemental Data Set 7. GO Biological Process Terms Significantly Overrepresented in Genes Rhythmically Expressed in the Mock-Inoculated Leaves.

Supplemental Data Set 8. GO Biological Process Terms Significantly Overrepresented in Genes Rhythmically Expressed in the Mock-Inoculated Leaves Grouped According to their Time of Peak Expression.

Supplemental Data Set 9. Known DNA Sequence Motif Enrichment in Gene Expression Clusters.

Supplemental Data Set 10. Transcription Factor Family Analysis Data.

Supplemental Data Set 11. Lists of Genes Differentially Expressed in *tga3-2* and the Time Series after *B. cinerea* Infection.

Supplemental Data Set 12. Potential Direct Target Genes of TGA3.

ACKNOWLEDGMENTS

O.W., E.B., and C.Z. were funded by a Biotechnology and Biological Sciences Research Council (BBSRC) core strategic grant to Warwick HRI. S.M., S.J.K., and R.H. were funded by the Engineering and Physical Sciences Research Council (EPSRC)/BBSRC funded Warwick Systems Biology Doctoral Training Centre. J.R. was funded by a BBSRC Systems Approaches to Biological Research studentship. J.B., K.J.D., V.B.-W., D.R., D.L.W., S.O., C.H., Y.-S.K., C.A.P., D.J.J., J.M., R.L., A.T., B.F., and L.B. are part of the BBRSC-funded grant Plant Response to Environmental Stress *Arabidopsis* (BB/F005806/1). P.M. was funded by a L'Oréal-UNESCO For Women In Science Fellowship and E.C. by the EPSRC-funded Molecular Organization and Assembly in Cells Doctoral Training Centre. S.A. and D.J.K. were supported by National Science Foundation IOS Award 1021861.

AUTHOR CONTRIBUTIONS

O.W., P.M., E.B., C.Z., and A.T. carried out experiments. S.M., R.L., J.M., and A.M. processed the data. O.S., K.B., C.H., E.C., R.H., S.J.K., J.R., D.J.J., C.A.P., L.B., S.A., D.J.K., Y.-S.K., O.W., V.B.-W., and K.J.D. were responsible for data analysis. A.M., B.F., D.L.W., D.R., J.B., S.O., V.B.-W, and K.J.D. all had input into the design of the experiments and analysis. K.J.D. wrote the article with contributions from all authors.

Received June 29, 2012; revised August 14, 2012; accepted September 7, 2012; published September 28, 2012.

REFERENCES

Abe, H., Urao, T., Ito, T., Seki, M., Shinozaki, K., and Yamaguchi-Shinozaki, K. (2003). *Arabidopsis* AtMYC2 (bHLH) and AtMYB2 (MYB) function as transcriptional activators in abscisic acid signaling. Plant Cell **15:** 63–78.

AbuQamar, S., Chen, X., Dhawan, R., Bluhm, B., Salmeron, J., Lam, S., Dietrich, R.A., and Mengiste, T. (2006). Expression profiling and mutant analysis reveals complex regulatory networks involved in *Arabidopsis* response to Botrytis infection. Plant J. **48:** 28–44.

Adhikari, N.D., Froehlich, J.E., Strand, D.D., Buck, S.M., Kramer, D.M., and Larkin, R.M. (2011). GUN4-porphyrin complexes bind the ChlH/GUN5 subunit of Mg-Chelatase and promote chlorophyll biosynthesis in *Arabidopsis*. Plant Cell **23:** 1449–1467.

Adie, B.A.T., Pérez-Pérez, J., Pérez-Pérez, M.M., Godoy, M., Sánchez-Serrano, J.-J., Schmelz, E.A., and Solano, R. (2007). ABA is an essential signal for plant resistance to pathogens affecting JA biosynthesis and the activation of defenses in *Arabidopsis*. Plant Cell **19:** 1665–1681.

Aggarwal, P., Padmanabhan, B., Bhat, A., Sarvepalli, K., Sadhale, P.P., and Nath, U. (2011). The TCP4 transcription factor of *Arabidopsis* blocks cell division in yeast at G1→S transition. Biochem. Biophys. Res. Commun. **410:** 276–281.

Amselem, J., et al. (2011). Genomic analysis of the necrotrophic fungal pathogens *Sclerotinia sclerotiorum* and *Botrytis cinerea*. PLoS Genet. **7:** e1002230.

Ashburner, M., et al; The Gene Ontology Consortium (2000). Gene ontology: Tool for the unification of biology. Nat. Genet. **25:** 25–29.

Asselbergh, B., De Vleesschauwer, D., and Höfte, M. (2008). Global switches and fine-tuning-ABA modulates plant pathogen defense. Mol. Plant Microbe Interact. **21:** 709–719.

Audenaert, K., De Meyer, G.B., and Höfte, M.M. (2002). Abscisic acid determines basal susceptibility of tomato to *Botrytis cinerea* and suppresses salicylic acid-dependent signaling mechanisms. Plant Physiol. **128:** 491–501.

Bellafiore, S., Barneche, F., Peltier, G., and Rochaix, J.-D. (2005). State transitions and light adaptation require chloroplast thylakoid protein kinase STN7. Nature **433:** 892–895.

Benjamini, Y., and Hochberg, Y. (1995). Controlling the false discovery rate: A practical and powerful approach to multiple testing. J. R. Stat. Soc. B **57:** 289–300.

Berrocal-Lobo, M., Molina, A., and Solano, R. (2002). Constitutive expression of *ETHYLENE-RESPONSE-FACTOR1* in *Arabidopsis* confers resistance to several necrotrophic fungi. Plant J. **29:** 23–32.

Bilgin, D.D., Zavala, J.A., Zhu, J., Clough, S.J., Ort, D.R., and DeLucia, E.H. (2010). Biotic stress globally downregulates photosynthesis genes. Plant Cell Environ. **33:** 1597–1613.

Birkenbihl, R.P., Diezel, C., and Somssich, I.E. (2012). *Arabidopsis* WRKY33 is a key transcriptional regulator of hormonal and metabolic responses toward *Botrytis cinerea* infection. Plant Physiol. **159:** 266–285.

Boller, T., and Felix, G. (2009). A renaissance of elicitors: Perception of microbe-associated molecular patterns and danger signals by pattern-recognition receptors. Annu. Rev. Plant Biol. **60:** 379–406.

Bonardi, V., Pesaresi, P., Becker, T., Schleiff, E., Wagner, R., Pfannschmidt, T., Jahns, P., and Leister, D. (2005). Photosystem II core phosphorylation and photosynthetic acclimation require two different protein kinases. Nature **437:** 1179–1182.

Boutrot, F., Chantret, N., and Gautier, M.-F. (2008). Genome-wide analysis of the rice and *Arabidopsis* non-specific lipid transfer protein (nsLtp) gene families and identification of wheat nsLtp genes by EST data mining. BMC Genomics **9:** 86.

Breeze, E., et al. (2011). High-resolution temporal profiling of transcripts during *Arabidopsis* leaf senescence reveals a distinct chronology of processes and regulation. Plant Cell **23:** 873–894.

Brutus, A., Sicilia, F., Macone, A., Cervone, F., and De Lorenzo, G. (2010). A domain swap approach reveals a role of the plant wall-associated kinase 1 (WAK1) as a receptor of oligogalacturonides. Proc. Natl. Acad. Sci. USA **107:** 9452–9457.

Bu, Q., Jiang, H., Li, C.-B., Zhai, Q., Zhang, J., Wu, X., Sun, J., Xie, Q., and Li, C. (2008). Role of the *Arabidopsis thaliana* NAC transcription factors ANAC019 and ANAC055 in regulating jasmonic acid-signaled defense responses. Cell Res. **18:** 756–767.

Cantu, D., Vicente, A.R., Greve, L.C., Dewey, F.M., Bennett, A.B., Labavitch, J.M., and Powell, A.L.T. (2008). The intersection between cell wall disassembly, ripening, and fruit susceptibility to *Botrytis cinerea*. Proc. Natl. Acad. Sci. USA **105:** 859–864.

Caño-Delgado, A., Yin, Y., Yu, C., Vafeados, D., Mora-García, S., Cheng, J.-C., Nam, K.H., Li, J., and Chory, J. (2004). BRL1 and BRL3 are novel brassinosteroid receptors that function in vascular differentiation in *Arabidopsis*. Development **131:** 5341–5351.

Carviel, J.L., Al-Daoud, F., Neumann, M., Mohammad, A., Provart, N.J., Moeder, W., Yoshioka, K., and Cameron, R.K. (2009). Forward and reverse genetics to identify genes involved in the age-related resistance response in *Arabidopsis thaliana*. Mol. Plant Pathol. **10:** 621–634.

Chen, L., Zhang, L., and Yu, D. (2010). Wounding-induced WRKY8 is involved in basal defense in *Arabidopsis*. Mol. Plant Microbe Interact. **23:** 558–565.

Chini, A., Boter, M., and Solano, R. (2009). Plant oxylipins: COI1/JAZs/MYC2 as the core jasmonic acid-signalling module. FEBS J. **276:** 4682–4692.

Clay, N.K., Adio, A.M., Denoux, C., Jander, G., and Ausubel, F.M. (2009). Glucosinolate metabolites required for an *Arabidopsis* innate immune response. Science **323:** 95–101.

Covington, M.F., Maloof, J.N., Straume, M., Kay, S.A., and Harmer, S.L. (2008). Global transcriptome analysis reveals circadian regulation of key pathways in plant growth and development. Genome Biol. **9:** R130.

Dean, R., Van Kan, J.A., Pretorius, Z.A., Hammond-Kosack, K.E., Di Pietro, A., Spanu, P.D., Rudd, J.J., Dickman, M., Kahmann, R., Ellis, J., and Foster, G.D. (2012). The Top 10 fungal pathogens in molecular plant pathology. Mol. Plant Pathol. **13:** 414–430.

Delessert, C., Kazan, K., Wilson, I.W., Van Der Straeten, D., Manners, J., Dennis, E.S., and Dolferus, R. (2005). The transcription factor ATAF2 represses the expression of pathogenesis-related genes in *Arabidopsis*. Plant J. **43:** 745–757.

Denby, K.J., Kumar, P., and Kliebenstein, D.J. (2004). Identification of *Botrytis cinerea* susceptibility loci in *Arabidopsis thaliana*. Plant J. **38:** 473–486.

Denoux, C., Galletti, R., Mammarella, N., Gopalan, S., Werck, D., De Lorenzo, G., Ferrari, S., Ausubel, F.M., and Dewdney, J. (2008). Activation of defense response pathways by OGs and Flg22 elicitors in *Arabidopsis* seedlings. Mol. Plant **1:** 423–445.

Dhawan, R., Luo, H., Foerster, A.M., Abuqamar, S., Du, H.-N., Briggs, S.D., Mittelsten Scheid, O., and Mengiste, T. (2009). HISTONE MONOUBIQUITINATION1 interacts with a subunit of the mediator complex and regulates defense against necrotrophic fungal pathogens in *Arabidopsis*. Plant Cell **21:** 1000–1019.

Dixon, D.P., and Edwards, R. (2009). Selective binding of glutathione conjugates of fatty acid derivatives by plant glutathione transferases. J. Biol. Chem. **284:** 21249–21256.

Dombrecht, B., Xue, G.P., Sprague, S.J., Kirkegaard, J.A., Ross, J.J., Reid, J.B., Fitt, G.P., Sewelam, N., Schenk, P.M., Manners, J.M., and Kazan, K. (2007). MYC2 differentially modulates diverse jasmonate-dependent functions in *Arabidopsis*. Plant Cell **19:** 2225–2245.

Donald, R.G., and Cashmore, A.R. (1990). Mutation of either G box or I box sequences profoundly affects expression from the *Arabidopsis* rbcS-1A promoter. EMBO J. **9:** 1717–1726.

Drechsel, G., Raab, S., and Hoth, S. (2010). *Arabidopsis* zinc-finger protein 2 is a negative regulator of ABA signaling during seed germination. J. Plant Physiol. **167:** 1418–1421.

Eklund, D.M., Ståldal, V., Valsecchi, I., Cierlik, I., Eriksson, C., Hiratsu, K., Ohme-Takagi, M., Sundström, J.F., Thelander, M., Ezcurra, I., and Sundberg, E. (2010). The *Arabidopsis thaliana* STYLISH1 protein acts as a transcriptional activator regulating auxin biosynthesis. Plant Cell **22:** 349–363.

Ellis, C., Karafyllidis, I., Wasternack, C., and Turner, J.G. (2002). The *Arabidopsis* mutant *cev1* links cell wall signaling to jasmonate and ethylene responses. Plant Cell **14:** 1557–1566.

Encinas-Villarejo, S., Maldonado, A.M., Amil-Ruiz, F., de los Santos, B., Romero, F., Pliego-Alfaro, F., Muñoz-Blanco, J., and Caballero, J.L. (2009). Evidence for a positive regulatory role of strawberry (*Fragaria* x *ananassa*) Fa WRKY1 and *Arabidopsis* At WRKY75 proteins in resistance. J. Exp. Bot. **60:** 3043–3065.

Eulgem, T., and Somssich, I.E. (2007). Networks of WRKY transcription factors in defense signaling. Curr. Opin. Plant Biol. **10:** 366–371.

Ferrari, S., Galletti, R., Denoux, C., De Lorenzo, G., Ausubel, F.M., and Dewdney, J. (2007). Resistance to *Botrytis cinerea* induced in *Arabidopsis* by elicitors is independent of salicylic acid, ethylene, or jasmonate signaling but requires PHYTOALEXIN DEFICIENT3. Plant Physiol. **144:** 367–379.

Ferrari, S., Plotnikova, J.M., De Lorenzo, G., and Ausubel, F.M. (2003). *Arabidopsis* local resistance to *Botrytis cinerea* involves salicylic acid and camalexin and requires EDS4 and PAD2, but not SID2, EDS5 or PAD4. Plant J. **35:** 193–205.

Fujita, M., Fujita, Y., Noutoshi, Y., Takahashi, F., Narusaka, Y., Yamaguchi-Shinozaki, K., and Shinozaki, K. (2006). Crosstalk between abiotic and biotic stress responses: A current view from the points of convergence in the stress signaling networks. Curr. Opin. Plant Biol. **9:** 436–442.

Galletti, R., Ferrari, S., and De Lorenzo, G. (2011). *Arabidopsis* MPK3 and MPK6 play different roles in basal and oligogalacturonide- or flagellin-induced resistance against *Botrytis cinerea*. Plant Physiol. **157:** 804–814.

Giraud, E., Ng, S., Carrie, C., Duncan, O., Low, J., Lee, C.P., Van Aken, O., Millar, A.H., Murcha, M., and Whelan, J. (2010). TCP transcription factors link the regulation of genes encoding mitochondrial proteins with the circadian clock in *Arabidopsis thaliana*. Plant Cell **22:** 3921–3934.

Govrin, E.M., and Levine, A. (2002). Infection of *Arabidopsis* with a necrotrophic pathogen, *Botrytis cinerea*, elicits various defense responses but does not induce systemic acquired resistance (SAR). Plant Mol. Biol. **48:** 267–276.

Govrin, E.M., Rachmilevitch, S., Tiwari, B.S., Solomon, M., and Levine, A. (2006). An elicitor from *Botrytis cinerea* induces the hypersensitive response in *Arabidopsis thaliana* and other plants and promotes the gray mold disease. Phytopathology **96:** 299–307.

Gutterson, N., and Reuber, T.L. (2004). Regulation of disease resistance pathways by AP2/ERF transcription factors. Curr. Opin. Plant Biol. **7:** 465–471.

Han, L., Li, G.-J., Yang, K.-Y., Mao, G., Wang, R., Liu, Y., and Zhang, S. (2010). Mitogen-activated protein kinase 3 and 6 regulate *Botrytis cinerea*-induced ethylene production in *Arabidopsis*. Plant J. **64:** 114–127.

Harmer, S.L., Hogenesch, J.B., Straume, M., Chang, H.S., Han, B., Zhu, T., Wang, X., Kreps, J.A., and Kay, S.A. (2000). Orchestrated transcription of key pathways in *Arabidopsis* by the circadian clock. Science **290:** 2110–2113.

Harmer, S.L., and Kay, S.A. (2005). Positive and negative factors confer phase-specific circadian regulation of transcription in *Arabidopsis*. Plant Cell **17:** 1926–1940.

Heard, N. (2011). Iterative reclassification in agglomerative clustering. J. Comput. Graph. Statist. **20:** 920–936.

Heard, N.A., Holmes, C.C., Stephens, D.A., Hand, D.J., and Dimopoulos, G. (2005). Bayesian coclustering of Anopheles gene expression time series: Study of immune defense response to multiple experimental challenges. Proc. Natl. Acad. Sci. USA **102:** 16939–16944.

Hervé, C., Dabos, P., Bardet, C., Jauneau, A., Auriac, M.-C., Ramboer, A., Lacout, F., and Tremousaygue, D. (2009). In vivo interference with AtTCP20 function induces severe plant growth alterations and deregulates the expression of many genes important for development. Plant Physiol. **149:** 1462–1477.

Hématy, K., Cherk, C., and Somerville, S. (2009). Host-pathogen warfare at the plant cell wall. Curr. Opin. Plant Biol. **12:** 406–413.

Hu, Y., Dong, Q., and Yu, D. (2012). *Arabidopsis* WRKY46 coordinates with WRKY70 and WRKY53 in basal resistance against pathogen *Pseudomonas syringae*. Plant Sci. **185-186:** 288–297.

Huang, M.-D., and Wu, W.-L. (2007). Overexpression of TMAC2, a novel negative regulator of abscisic acid and salinity responses, has pleiotropic effects in *Arabidopsis thaliana*. Plant Mol. Biol. **63:** 557–569.

Huffaker, A., Pearce, G., and Ryan, C.A. (2006). An endogenous peptide signal in *Arabidopsis* activates components of the innate immune response. Proc. Natl. Acad. Sci. USA **103:** 10098–10103.

Hughes, M.E., Hogenesch, J.B., and Kornacker, K. (2010). JTK_CYCLE: An efficient nonparametric algorithm for detecting rhythmic components in genome-scale data sets. J. Biol. Rhythms **25:** 372–380.

Huq, E., Al-Sady, B., Hudson, M., Kim, C., Apel, K., and Quail, P.H. (2004). Phytochrome-interacting factor 1 is a critical bHLH regulator of chlorophyll biosynthesis. Science **305:** 1937–1941.

Huq, E., and Quail, P.H. (2002). PIF4, a phytochrome-interacting bHLH factor, functions as a negative regulator of phytochrome B signaling in *Arabidopsis*. EMBO J. **21:** 2441–2450.

Johnson, C., Boden, E., and Arias, J. (2003). Salicylic acid and NPR1 induce the recruitment of trans-activating TGA factors to a defense gene promoter in *Arabidopsis*. Plant Cell **15:** 1846–1858.

Jones, J.D.G., and Dangl, J.L. (2006). The plant immune system. Nature **444:** 323–329.

Kaplan-Levy, R.N., Brewer, P.B., Quon, T., and Smyth, D.R. (2012). The trihelix family of transcription factors—Light, stress and development. Trends Plant Sci. **17:** 163–171.

Kel, A.E., Gössling, E., Reuter, I., Cheremushkin, E., Kel-Margoulis, O.V., and Wingender, E. (2003). MATCH: A tool for searching transcription factor binding sites in DNA sequences. Nucleic Acids Res. **31:** 3576–3579.

Kesarwani, M., Yoo, J., and Dong, X. (2007). Genetic interactions of TGA transcription factors in the regulation of pathogenesis-related genes and disease resistance in Arabidopsis. Plant Physiol. **144:** 336–346.

Kidokoro, S., Maruyama, K., Nakashima, K., Imura, Y., Narusaka, Y., Shinwari, Z.K., Osakabe, Y., Fujita, Y., Mizoi, J., Shinozaki, K., and Yamaguchi-Shinozaki, K. (2009). The phytochrome-interacting factor PIF7 negatively regulates DREB1 expression under circadian control in Arabidopsis. Plant Physiol. **151:** 2046–2057.

Kieffer, M., Master, V., Waites, R., and Davies, B. (2011). TCP14 and TCP15 affect internode length and leaf shape in *Arabidopsis*. Plant J. **68:** 147–158.

Klemm, S. (2008). Causal Structure Identification in Nonlinear Dynamical Systems. Master's thesis (Cambridge, UK: University of Cambridge).

Kliebenstein, D.J., Rowe, H.C., and Denby, K.J. (2005). Secondary metabolites influence *Arabidopsis*/Botrytis interactions: Variation in host production and pathogen sensitivity. Plant J. **44:** 25–36.

Knoth, C., Ringler, J., Dangl, J.L., and Eulgem, T. (2007). *Arabidopsis* WRKY70 is required for full RPP4-mediated disease resistance and basal defense against *Hyaloperonospora parasitica*. Mol. Plant Microbe Interact. **20:** 120–128.

Kunz, C., Vandelle, E., Rolland, S., Poinssot, B., Bruel, C., Cimerman, A., Zotti, C., Moreau, E., Vedel, R., Pugin, A., and Boccara, M. (2006). Characterization of a new, nonpathogenic mutant of *Botrytis cinerea* with impaired plant colonization capacity. New Phytol. **170:** 537–550.

Kwon, C., et al. (2008). Co-option of a default secretory pathway for plant immune responses. Nature **451:** 835–840.

Lai, Z., Vinod, K., Zheng, Z., Fan, B., and Chen, Z. (2008). Roles of *Arabidopsis* WRKY3 and WRKY4 transcription factors in plant responses to pathogens. BMC Plant Biol. **8:** 68.

Lai, Z., Wang, F., Zheng, Z., Fan, B., and Chen, Z. (2011). A critical role of autophagy in plant resistance to necrotrophic fungal pathogens. Plant J. **66:** 953–968.

Laluk, K., Luo, H., Chai, M., Dhawan, R., Lai, Z., and Mengiste, T. (2011). Biochemical and genetic requirements for function of the immune response regulator BOTRYTIS-INDUCED KINASE1 in plant growth, ethylene signaling, and PAMP-triggered immunity in *Arabidopsis*. Plant Cell **23:** 2831–2849.

Lee, H., Fischer, R.L., Goldberg, R.B., and Harada, J.J. (2003). *Arabidopsis* LEAFY COTYLEDON1 represents a functionally specialized subunit of the CCAAT binding transcription factor. Proc. Natl. Acad. Sci. USA **100:** 2152–2156.

Li, C., Potuschak, T., Colón-Carmona, A., Gutiérrez, R.A., and Doerner, P. (2005). *Arabidopsis* TCP20 links regulation of growth and cell division control pathways. Proc. Natl. Acad. Sci. USA **102:** 12978–12983.

Li, J., Brader, G., Kariola, T., and Palva, E.T. (2006). WRKY70 modulates the selection of signaling pathways in plant defense. Plant J. **46:** 477–491.

Li, J., Wen, J., Lease, K.A., Doke, J.T., Tax, F.E., and Walker, J.C. (2002). BAK1, an *Arabidopsis* LRR receptor-like protein kinase, interacts with BRI1 and modulates brassinosteroid signaling. Cell **110:** 213–222.

Lionetti, V., Raiola, A., Camardella, L., Giovane, A., Obel, N., Pauly, M., Favaron, F., Cervone, F., and Bellincampi, D. (2007). Overexpression of pectin methylesterase inhibitors in *Arabidopsis* restricts fungal infection by *Botrytis cinerea*. Plant Physiol. **143:** 1871–1880.

Liu, J.-X., and Howell, S.H. (2010). bZIP28 and NF-Y transcription factors are activated by ER stress and assemble into a transcriptional complex to regulate stress response genes in *Arabidopsis*. Plant Cell **22:** 782–796.

Loake, G., and Grant, M. (2007). Salicylic acid in plant defence—The players and protagonists. Curr. Opin. Plant Biol. **10:** 466–472.

Lu, D., Wu, S., Gao, X., Zhang, Y., Shan, L., and He, P. (2010). A receptor-like cytoplasmic kinase, BIK1, associates with a flagellin receptor complex to initiate plant innate immunity. Proc. Natl. Acad. Sci. USA **107:** 496–501.

Luo, H., Laluk, K., Lai, Z., Veronese, P., Song, F., and Mengiste, T. (2010). The *Arabidopsis* Botrytis Susceptible1 Interactor defines a subclass of RING E3 ligases that regulate pathogen and stress responses. Plant Physiol. **154:** 1766–1782.

Maere, S., Heymans, K., and Kuiper, M. (2005). BiNGO: A Cytoscape plugin to assess overrepresentation of gene ontology categories in biological networks. Bioinformatics **21:** 3448–3449.

Manni, I., Caretti, G., Artuso, S., Gurtner, A., Emiliozzi, V., Sacchi, A., Mantovani, R., and Piaggio, G. (2008). Posttranslational regulation of NF-YA modulates NF-Y transcriptional activity. Mol. Biol. Cell **19:** 5203–5213.

Mao, G., Meng, X., Liu, Y., Zheng, Z., Chen, Z., and Zhang, S. (2011). Phosphorylation of a WRKY transcription factor by two pathogen-responsive MAPKs drives phytoalexin biosynthesis in *Arabidopsis*. Plant Cell **23:** 1639–1653.

Martín-Trillo, M., and Cubas, P. (2010). TCP genes: A family snapshot ten years later. Trends Plant Sci. **15:** 31–39.

Matys, V., et al. (2006). TRANSFAC and its module TRANSCompel: Transcriptional gene regulation in eukaryotes. Nucleic Acids Res. **34** (Database issue)**:** D108–D110.

Mengiste, T., Chen, X., Salmeron, J., and Dietrich, R. (2003). The BOTRYTIS SUSCEPTIBLE1 gene encodes an R2R3MYB transcription factor protein that is required for biotic and abiotic stress responses in *Arabidopsis*. Plant Cell **15:** 2551–2565.

Menkens, A.E., Schindler, U., and Cashmore, A.R. (1995). The G-box: A ubiquitous regulatory DNA element in plants bound by the GBF family of bZIP proteins. Trends Biochem. Sci. **20:** 506–510.

Mikkelsen, M.D., and Thomashow, M.F. (2009). A role for circadian evening elements in cold-regulated gene expression in *Arabidopsis*. Plant J. **60:** 328–339.

Moffat, C.S., Ingle, R.A., Wathugala, D.L., Saunders, N.J., Knight, H., and Knight, M.R. (2012). ERF5 and ERF6 play redundant roles as positive regulators of JA/Et-mediated defense against *Botrytis cinerea* in *Arabidopsis*. PLoS ONE **7:** e35995.

Motose, H., Sugiyama, M., and Fukuda, H. (2004). A proteoglycan mediates inductive interaction during plant vascular development. Nature **429:** 873–878.

Mulema, J.M.K., and Denby, K.J. (2012). Spatial and temporal transcriptomic analysis of the *Arabidopsis thaliana-Botrytis cinerea* interaction. Mol. Biol. Rep. **39:** 4039–4049.

Nakano, T., Suzuki, K., Fujimura, T., and Shinshi, H. (2006). Genome-wide analysis of the ERF gene family in Arabidopsis and rice. Plant Physiol. **140:** 411–432.

Nakashima, K., Takasaki, H., Mizoi, J., Shinozaki, K., and Yamaguchi-Shinozaki, K. (2012). NAC transcription factors in plant abiotic stress responses. Biochim. Biophys. Acta **1819:** 97–103.

Nawrath, C., Heck, S., Parinthawong, N., and Métraux, J.-P. (2002). EDS5, an essential component of salicylic acid-dependent signaling for disease resistance in *Arabidopsis*, is a member of the MATE transporter family. Plant Cell **14:** 275–286.

Okamoto, M., Kushiro, T., Jikumaru, Y., Abrams, S.R., Kamiya, Y., Seki, M., and Nambara, E. (2011). ABA 9′-hydroxylation is catalyzed by CYP707A in *Arabidopsis*. Phytochemistry **72:** 717–722.

Omote, H., Hiasa, M., Matsumoto, T., Otsuka, M., and Moriyama, Y. (2006). The MATE proteins as fundamental transporters of metabolic and xenobiotic organic cations. Trends Pharmacol. Sci. **27:** 587–593.

Palaniswamy, S.K., James, S., Sun, H., Lamb, R.S., Davuluri, R.V., and Grotewold, E. (2006). AGRIS and AtRegNet. a platform to link cis-regulatory elements and transcription factors into regulatory networks. Plant Physiol. **140:** 818–829.

Pandey, G.K., Grant, J.J., Cheong, Y.H., Kim, B.G., Li, L., and Luan, S. (2005). ABR1, an APETALA2-domain transcription factor that functions as a repressor of ABA response in Arabidopsis. Plant Physiol. **139:** 1185–1193.

Pandey, S.P., and Somssich, I.E. (2009). The role of WRKY transcription factors in plant immunity. Plant Physiol. **150:** 1648–1655.

Penfold, C., and Wild, D.L. (2011). How to infer gene networks from expression profiles, revisited. Interface Focus **1:** 857–870.

Pham, J., Liu, J., Bennett, M.H., Mansfield, J.W., and Desikan, R. (2012). *Arabidopsis* histidine kinase 5 regulates salt sensitivity and resistance against bacterial and fungal infection. New Phytol. **194:** 168–180.

Poinssot, B., Vandelle, E., Bentéjac, M., Adrian, M., Levis, C., Brygoo, Y., Garin, J., Sicilia, F., Coutos-Thévenot, P., and Pugin, A. (2003). The endopolygalacturonase 1 from *Botrytis cinerea* activates grapevine defense reactions unrelated to its enzymatic activity. Mol. Plant Microbe Interact. **16:** 553–564.

Pré, M., Atallah, M., Champion, A., De Vos, M., Pieterse, C.M.J., and Memelink, J. (2008). The AP2/ERF domain transcription factor ORA59 integrates jasmonic acid and ethylene signals in plant defense. Plant Physiol. **147:** 1347–1357.

Priest, D.M., Jackson, R.G., Ashford, D.A., Abrams, S.R., and Bowles, D.J. (2005). The use of abscisic acid analogues to analyse the substrate selectivity of UGT71B6, a UDP-glycosyltransferase of *Arabidopsis thaliana*. FEBS Lett. **579:** 4454–4458.

Pruneda-Paz, J.L., Breton, G., Para, A., and Kay, S.A. (2009). A functional genomics approach reveals CHE as a component of the *Arabidopsis* circadian clock. Science **323:** 1481–1485.

Qiu, J.-L., et al. (2008). *Arabidopsis* MAP kinase 4 regulates gene expression through transcription factor release in the nucleus. EMBO J. **27:** 2214–2221.

Ramírez, V., Agorio, A., Coego, A., García-Andrade, J., Hernández, M.J., Balaguer, B., Ouwerkerk, P.B.F., Zarra, I., and Vera, P. (2011a). MYB46 modulates disease susceptibility to *Botrytis cinerea* in Arabidopsis. Plant Physiol. **155:** 1920–1935.

Ramírez, V., García-Andrade, J., and Vera, P. (2011b). Enhanced disease resistance to *Botrytis cinerea* in *myb46 Arabidopsis* plants is associated to an early down-regulation of CesA genes. Plant Signal. Behav. **6:** 911–913.

Rasmussen, C.E., and Williams, C.K.I. (2006). Gaussian Processes for Machine Learning. (Cambridge, MA: The MIT Press).

Roden, L.C., and Ingle, R.A. (2009). Lights, rhythms, infection: The role of light and the circadian clock in determining the outcome of plant-pathogen interactions. Plant Cell **21:** 2546–2552.

Roux, M., Schwessinger, B., Albrecht, C., Chinchilla, D., Jones, A., Holton, N., Malinovsky, F.G., Tör, M., de Vries, S., and Zipfel, C. (2011). The *Arabidopsis* leucine-rich repeat receptor-like kinases BAK1/SERK3 and BKK1/SERK4 are required for innate immunity to hemibiotrophic and biotrophic pathogens. Plant Cell **23:** 2440–2455.

Rowe, H.C., Walley, J.W., Corwin, J., Chan, E.K.F., Dehesh, K., and Kliebenstein, D.J. (2010). Deficiencies in jasmonate-mediated plant defense reveal quantitative variation in *Botrytis cinerea* pathogenesis. PLoS Pathog. **6:** e1000861.

Saito, S., Hirai, N., Matsumoto, C., Ohigashi, H., Ohta, D., Sakata, K., and Mizutani, M. (2004). *Arabidopsis* CYP707As encode (+)-abscisic acid 8′-hydroxylase, a key enzyme in the oxidative catabolism of abscisic acid. Plant Physiol. **134:** 1439–1449.

Sato, M., Tsuda, K., Wang, L., Coller, J., Watanabe, Y., Glazebrook, J., and Katagiri, F. (2010). Network modeling reveals prevalent negative regulatory relationships between signaling sectors in *Arabidopsis* immune signaling. PLoS Pathog. **6:** e1001011.

Sauerbrunn, N., and Schlaich, N.L. (2004). PCC1: A merging point for pathogen defence and circadian signalling in *Arabidopsis*. Planta **218:** 552–561.

Schommer, C., Palatnik, J.F., Aggarwal, P., Chételat, A., Cubas, P., Farmer, E.E., Nath, U., and Weigel, D. (2008). Control of jasmonate biosynthesis and senescence by miR319 targets. PLoS Biol. **6:** e230.

Sclep, G., Allemeersch, J., Liechti, R., De Meyer, B., Beynon, J., Bhalerao, R., Moreau, Y., Nietfeld, W., Renou, J.-P., Reymond, P., Kuiper, M.T., and Hilson, P. (2007). CATMA, a comprehensive genome-scale resource for silencing and transcript profiling of *Arabidopsis* genes. BMC Bioinformatics **8:** 400.

Shin, J., Kim, K., Kang, H., Zulfugarov, I.S., Bae, G., Lee, C.-H., Lee, D., and Choi, G. (2009). Phytochromes promote seedling light responses by inhibiting four negatively-acting phytochrome-interacting factors. Proc. Natl. Acad. Sci. USA **106:** 7660–7665.

Siewers, V., Kokkelink, L., Smedsgaard, J., and Tudzynski, P. (2006). Identification of an abscisic acid gene cluster in the grey mold *Botrytis cinerea*. Appl. Environ. Microbiol. **72:** 4619–4626.

Skirycz, A., Reichelt, M., Burow, M., Birkemeyer, C., Rolcik, J., Kopka, J., Zanor, M.I., Gershenzon, J., Strnad, M., Szopa, J., Mueller-Roeber, B., and Witt, I. (2006). DOF transcription factor AtDof1.1 (OBP2) is part of a regulatory network controlling glucosinolate biosynthesis in *Arabidopsis*. Plant J. **47:** 10–24.

Son, G.H., Wan, J., Kim, H.J., Nguyen, X.C., Chung, W.S., Hong, J.C., and Stacey, G. (2012). Ethylene-responsive element-binding factor 5, ERF5, is involved in chitin-induced innate immunity response. Mol. Plant Microbe Interact. **25:** 48–60.

Stegle, O., Denby, K.J., Cooke, E.J., Wild, D.L., Ghahramani, Z., and Borgwardt, K.M. (2010). A robust Bayesian two-sample test for detecting intervals of differential gene expression in microarray time series. J. Comput. Biol. **17:** 355–367.

Stepanova, A.N., Hoyt, J.M., Hamilton, A.A., and Alonso, J.M. (2005). A Link between ethylene and auxin uncovered by the characterization of two root-specific ethylene-insensitive mutants in *Arabidopsis*. Plant Cell **17:** 2230–2242.

Stracke, R., Werber, M., and Weisshaar, B. (2001). The R2R3-MYB gene family in *Arabidopsis thaliana*. Curr. Opin. Plant Biol. **4:** 447–456.

Sun, X., Gilroy, E.M., Chini, A., Nurmberg, P.L., Hein, I., Lacomme, C., Birch, P.R.J., Hussain, A., Yun, B.-W., and Loake, G.J. (2011). ADS1 encodes a MATE-transporter that negatively regulates plant disease resistance. New Phytol. **192:** 471–482.

Sønderby, I.E., Hansen, B.G., Bjarnholt, N., Ticconi, C., Halkier, B.A., and Kliebenstein, D.J. (2007). A systems biology approach identifies a R2R3 MYB gene subfamily with distinct and overlapping functions in regulation of aliphatic glucosinolates. PLoS ONE **2:** e1322.

Tai, Y.C., and Speed, T.P. (2006). A multivariate empirical Bayes statistic for replicated microarray time course data. Annal. Stat. **34:** 2387–2412.

Thomma, B.P., Eggermont, K., Penninckx, I.A., Mauch-Mani, B., Vogelsang, R., Cammue, B.P., and Broekaert, W.F. (1998). Separate jasmonate-dependent and salicylate-dependent defense-response pathways in *Arabidopsis* are essential for resistance to distinct microbial pathogens. Proc. Natl. Acad. Sci. USA **95:** 15107–15111.

Thomma, B.P., Eggermont, K., Tierens, K.F., and Broekaert, W.F. (1999). Requirement of functional ethylene-insensitive 2 gene for efficient resistance of Arabidopsis to infection by *Botrytis cinerea*. Plant Physiol. **121:** 1093–1102.

Ton, J., Flors, V., and Mauch-Mani, B. (2009). The multifaceted role of ABA in disease resistance. Trends Plant Sci. **14:** 310–317.

Tsuchisaka, A., and Theologis, A. (2004). Unique and overlapping expression patterns among the Arabidopsis 1-amino-cyclopropane-1-carboxylate synthase gene family members. Plant Physiol. **136:** 2982–3000.

van Loon, L., and van Strien, E. (1999). The families of pathogenesis-related proteins, their activities, and comparative analysis of PR-1 type proteins. Physiol. Mol. Plant Pathol. **55:** 85–97.

Verhage, A., van Wees, S.C.M., and Pieterse, C.M.J. (2010). Plant immunity: It's the hormones talking, but what do they say? Plant Physiol. **154:** 536–540.

Wang, W., Barnaby, J.Y., Tada, Y., Li, H., Tör, M., Caldelari, D., Lee, D.-U., Fu, X.-D., and Dong, X. (2011). Timing of plant immune responses by a central circadian regulator. Nature **470:** 110–114.

Wang, X., Basnayake, B.M.V.S., Zhang, H., Li, G., Li, W., Virk, N., Mengiste, T., and Song, F. (2009). The *Arabidopsis* ATAF1, a NAC transcription factor, is a negative regulator of defense responses against necrotrophic fungal and bacterial pathogens. Mol. Plant Microbe Interact. **22:** 1227–1238.

Wenkel, S., Turck, F., Singer, K., Gissot, L., Le Gourrierec, J., Samach, A., and Coupland, G. (2006). CONSTANS and the CCAAT box binding complex share a functionally important domain and interact to regulate flowering of *Arabidopsis*. Plant Cell **18:** 2971–2984.

Wettenhall, J.M., and Smyth, G.K. (2004). limmaGUI: A graphical user interface for linear modeling of microarray data. Bioinformatics **20:** 3705–3706.

Whalley, H.J., Sargeant, A.W., Steele, J.F.C., Lacoere, T., Lamb, R., Saunders, N.J., Knight, H., and Knight, M.R. (2011). Transcriptomic analysis reveals calcium regulation of specific promoter motifs in *Arabidopsis*. Plant Cell **23:** 4079–4095.

Williamson, B., Tudzynski, B., Tudzynski, P., and van Kan, J.A.L. (2007). *Botrytis cinerea*: The cause of grey mould disease. Mol. Plant Pathol. **8:** 561–580.

Wu, H., Kerr, K., Cui, X., and Churchill, G. (2003). MAANOVA: A software package for the analysis of spotted cDNA microarray experiments. In The Analysis of Gene Expression Data: Methods and Software, G. Parmigiani, E. Garrett, R. Irizarry, and S. Zeger, eds. (New York: Springer), pp. 313–341.

Wu, Y., Deng, Z., Lai, J., Zhang, Y., Yang, C., Yin, B., Zhao, Q., Zhang, L., Li, Y., Yang, C., and Xie, Q. (2009). Dual function of *Arabidopsis* ATAF1 in abiotic and biotic stress responses. Cell Res. **19:** 1279–1290.

Xu, X., Chen, C., Fan, B., and Chen, Z. (2006). Physical and functional interactions between pathogen-induced *Arabidopsis* WRKY18, WRKY40, and WRKY60 transcription factors. Plant Cell **18:** 1310–1326.

Yanagisawa, S. (2004). Dof domain proteins: Plant-specific transcription factors associated with diverse phenomena unique to plants. Plant Cell Physiol. **45:** 386–391.

Yang, Z., Tian, L., Latoszek-Green, M., Brown, D., and Wu, K. (2005). *Arabidopsis* ERF4 is a transcriptional repressor capable of modulating ethylene and abscisic acid responses. Plant Mol. Biol. **58:** 585–596.

Yin, X.J., et al. (2007). Ubiquitin lysine 63 chain forming ligases regulate apical dominance in *Arabidopsis*. Plant Cell **19:** 1898–1911.

Zander, M., La Camera, S., Lamotte, O., Métraux, J.-P., and Gatz, C. (2010). *Arabidopsis thaliana* class-II TGA transcription factors are essential activators of jasmonic acid/ethylene-induced defense responses. Plant J. **61:** 200–210.

Zhang, J., et al. (2010). Receptor-like cytoplasmic kinases integrate signaling from multiple plant immune receptors and are targeted by a *Pseudomonas syringae* effector. Cell Host Microbe **7:** 290–301.

Zhang, Y., Tessaro, M.J., Lassner, M., and Li, X. (2003). Knockout analysis of *Arabidopsis* transcription factors TGA2, TGA5, and TGA6 reveals their redundant and essential roles in systemic acquired resistance. Plant Cell **15:** 2647–2653.

Zhao, Y., Wei, T., Yin, K.-Q., Chen, Z., Gu, H., Qu, L.-J., and Qin, G. (2012). *Arabidopsis* RAP2.2 plays an important role in plant resistance to *Botrytis cinerea* and ethylene responses. New Phytol. **195:** 450–460.

Zhong, R., Lee, C., Zhou, J., McCarthy, R.L., and Ye, Z.-H. (2008). A battery of transcription factors involved in the regulation of secondary cell wall biosynthesis in *Arabidopsis*. Plant Cell **20:** 2763–2782.

Zimmerli, L., Métraux, J.P., and Mauch-Mani, B. (2001). Beta-aminobutyric acid-induced protection of Arabidopsis against the necrotrophic fungus *Botrytis cinerea*. Plant Physiol. **126:** 517–523.

Arabidopsis Defense against *Botrytis cinerea*: Chronology and Regulation Deciphered by High-Resolution Temporal Transcriptomic Analysis

Oliver Windram, Priyadharshini Madhou, Stuart McHattie, Claire Hill, Richard Hickman, Emma Cooke, Dafyd J. Jenkins, Christopher A. Penfold, Laura Baxter, Emily Breeze, Steven J. Kiddle, Johanna Rhodes, Susanna Atwell, Daniel J. Kliebenstein, Youn-sung Kim, Oliver Stegle, Karsten Borgwardt, Cunjin Zhang, Alex Tabrett, Roxane Legaie, Jonathan Moore, Bärbel Finkenstadt, David L. Wild, Andrew Mead, David Rand, Jim Beynon, Sascha Ott, Vicky Buchanan-Wollaston and Katherine J. Denby

Plant Cell; originally published online September 28, 2012;
DOI 10.1105/tpc.112.102046